Batteries & Supercaps

Perspective
doi.org/10.1002/batt.202500359

Chemistry Europe
European Chemical Societies Publishing

www.batteries-supercaps.org

Carbon-Based Electrodes: Harnessing Organic Compound Oxidation for Sustainable Redox Flow Batteries

Zheng Tang, Yifan Zhang,* Wulin Yang,* Zipeng Zhao,* and Jincai Zhao

Carbon-based materials, due to their natural abundance, high conductivity, tunable surface chemistry, and good stability, have emerged as a material choice in the electrochemical advanced oxidation processes (EAOPs) for catalytic degradation of organic compounds. Recent progress is summarized from the perspective of materials design and engineering. Specifically, the fundamental mechanisms underlying EAOPs are introduced, with a focus on the activation of hydrogen peroxide, peroxymonosulfate, and peroxydisulfate to generate reactive species essential for organic contaminants degradation in wastewater. Additionally, various materials engineering strategies and their associated structure-property relationships are examined, including the optimization of morphology, surface functional group modification, and elemental doping. The reviewed materials are categorized based on their suitability for specific applications, such as electro-Fenton, heterogeneous electro-Fenton, and nonelectro-Fenton processes. Furthermore, strategies for enhancing the overall performance of EAOP systems are discussed, including the design of bipolar electrodes and the integration of external fields, such as microwaves, to accelerate EAOP reactions through the modulation of electrode potentials. Finally, the perspective outlines the opportunities, challenges, and future directions of carbon-based materials in the catalytic field of EAOPs. In addition, the perspective examines the potential and hurdles of carbon-based electrodes in sustainable redox flow batteries, outlining pathways toward efficient, sustainable water treatment.

1. Introduction

Currently, untreated industrial wastewater introduces various organic compounds into aquatic ecosystems, such as medicines, pesticides, dyes, and petrochemical products.[1] In recent years, a variety of methods have been explored for the treatment of organic pollutants. These approaches include membrane separation, adsorption, advanced oxidation processes (AOPs), and biological techniques such as activated sludge systems and membrane bioreactors.[2]

Z. Tang
Tianfu Yongxing Laboratory
Chengdu 610213, China

Z. Tang, Z. Zhao
Beijing Key Laboratory of Construction Tailorable Advanced Functional Materials and Green Applications
Experimental Center of Advanced Materials
School of Materials Science and Engineering
Beijing Institute of Technology
Beijing 100081, China
E-mail: zipengzhao@bit.edu.cn

Y. Zhang, J. Zhao
Key Laboratory of Photochemistry
CAS Research/Education Center for Excellence in Molecular Sciences
Institute of Chemistry
Chinese Academy of Sciences
Beijing 100190, China
E-mail: yfzhang@iccas.ac.cn

W. Yang
College of Environmental Sciences and Engineering
Peking University
Beijing 100871, China
E-mail: wulin.yang@pku.edu.cn

Among the above treatment methods, AOPs stand out as a leading and promising technology for addressing the issue induced by organic pollutants. These processes involve the catalytic decomposition of peroxides, such as hydrogen peroxide or persulfates, which leads to the generation of reactive free radicals [e.g. hydroxyl radicals (•OH) and sulfate radical anion (SO_4•$^-$)] as well as nonradical species like singlet oxygen ($^1O_2$).[3] Compared to conventional AOPs that rely on energy-intensive processes such as photolysis, sonolysis, and thermal decomposition for precursor activation, electrochemical advanced oxidation processes (EAOPs) utilize an electric potential to directly drive redox reactions, thereby achieving superior energy efficiency.[4,5] Notably, under optimized operational conditions, EAOPs demonstrate significant cost-efficiency benefits, particularly when integrated with renewable energy sources like wind and solar power.[6] Thus, EAOPs have become a promising alternative to traditional AOPs for the removal of organic pollutants from wastewater.[7]

Carbon-based materials play a crucial role in the EAOPs.[8] Specifically, carbon-based materials like graphene, carbon nanotubes, activated carbon, and biochar, along with their composites, offer distinct advantages in EAOPs. These include high electrical conductivity, a large specific surface area, and tunable surface chemical properties. Notably, carbon-based materials display remarkable efficiency in catalyzing the decomposition of peroxides (e.g., H_2O_2 and persulfates) to produce reactive oxygen species (ROS) (e.g., •OH and SO_4•$^-$) for degradation of organic pollutants in wastewater.[9]

Although there have been some reviews on the applications of carbon-based materials in EAOPs.[10,11] Specifically, Liu et al. systematically reviewed the physical and chemical properties of biochar as a catalyst and electrode material in the EAOPs.[10]

Their study not only explored various techniques to optimize these properties but also provided an in-depth analysis of the mechanisms underlying the electrocatalytic in situ generation and activation of H_2O_2 by biochar-based materials. Furthermore, Guo et al. reviewed recent advancements in nitrogen-doped carbon-based catalysts as cathodes in EAOPs, emphasizing their role in improving oxygen reduction reaction (ORR) activity, H_2O_2 selectivity, and •OH yield.[11] Their study also provided a detailed discussion of the influence of different nitrogen configurations on two-electron-ORR and •OH generation, as well as the synergistic effects of codoping nitrogen with other heteroatoms [e.g., fluorine (F), phosphorus (P), sulfur (S), and oxygen (O)] on two-electron-ORR. These articles provide an overview, focusing on specific categories of carbon-based materials and their significant role in the field of EAOPs. Note that carbon-based materials combined with metal catalysts, such as metal nanoparticles, metal oxide nanoparticles, and metal-based single-atom catalysts (SACs), also play a crucial role in EAOPs, often demonstrating superior performance in terms of activity and stability. However, there is no systematic discussion and summarization about those catalysts. In addition, research on generating reactive species via the activation of persulfates using carbon-based materials in EAOPs for the oxidative degradation of organic pollutants has not yet been systematically discussed.

Herein, we discuss the design of carbon-based materials (with or without metal contents) and their application as catalysts in EAOPs. Specifically, we discussed the mechanism of generating ROS via activating H_2O_2, peroxymonosulfate (PMS), and peroxydisulfate (PDS). Then, we discuss the recent progress in EAOP from the perspective of materials design and structure-property relationship. Furthermore, we also summarize strategies for improving the organic compound degradation efficiency and energy efficiency with designed materials, including improving electrode design and introducing external fields (e.g., microwave). Additionally, the theoretically possible flow battery configuration is discussed, which employs the positive electrode capable of in situ generation of H_2O_2 for EAOP. This device can be used for both purifying water and generating electricity simultaneously. Finally, we highlight the challenges and future research trends for carbon-based materials, such as materials optimization and cost reduction for broad applications.

2. The Formation Mechanisms of Reactive Species in Organic Wastewater during EAOPs

The EAOPs stand as a highly efficient wastewater treatment technology that has undergone significant advancements. Within this method, ROS generated by electrocatalysis are capable of oxidizing and breaking down diverse organic pollutants and producing unharmful molecules like CO_2, H_2O, and inorganic ions, like sulfate, nitrate, and ammonium.[12] Moreover, these oxygen species exhibit robust environmental compatibility by employing an exceptionally clean reagent—electrons.[13,14] Significantly, peroxide-based EAOPs are an effective method for enhancing the concentration of generated radicals (such as •OH and $SO_4^{\bullet-}$) and accelerating the degradation of organic pollutants in aqueous systems.[15] In this section, we introduce the peroxide-based EAOPs with different peroxides (such as H_2O_2, PMS, and PDS) and elaborate on the reaction mechanisms of EAOPs combined with various peroxides in detail, for organic pollutant degradation.

2.1. Hydrogen-Peroxide-Based EAOPs

Research findings indicate that EAOPs based on H_2O_2 have garnered widespread application in pollutant degradation technologies, due to cost-effectiveness, environmental friendliness, and nonpolluting attributes of H_2O_2.[10] Within this system, organic pollutants can undergo oxidative degradation via direct, quasidirect, and indirect pathways in EAOPs. In the direct pathway, organic pollutants are oxidized through direct electron transfer at the surface of the anode.[16] In the quasidirect pathway, organic pollutants react with hydroxyl radicals (•OH) that are generated from the anodic water oxidation reaction occurring at the anode surface (M).[17,18] The reaction equation is as follows (Equation (1)).[16]

$$M + H_2O \rightarrow M(\bullet OH) + H^+ + e^- \quad (1)$$

As for the indirect pathway, it specifically involves the reduction of O_2 at the cathode via a two-electron ORR, producing H_2O_2. This H_2O_2 is subsequently activated to generate •OH, which then oxidizes and degrades the organic pollutants.[19] We mainly discuss the mechanism of activating H_2O_2 on the cathode side, which involves two main pathways. The first pathway is the electro-Fenton process, where Fe^{2+} activates in situ-generated H_2O_2 to produce •OH. The second pathway involves the direct activation of H_2O_2 by the cathodic catalyst to produce •OH radicals.[20,21]

The following is the reaction mechanism and corresponding equations of the electro-Fenton process (Equation (2–4)).[20,21] Specifically, oxygen is first reduced at the cathode surface by gaining two electrons to form H_2O_2. Subsequently, H_2O_2 is activated by Fe^{2+}, thus generating •OH and Fe^{3+}. Finally, Fe^{2+} is regenerated at the cathode by electron transfer.

$$O_2 + 2H^+ + 2e^- \rightarrow H_2O_2 \quad (2)$$

$$H_2O_2 + Fe^{2+} \rightarrow Fe^{3+} + OH^- + \bullet OH \quad (3)$$

$$Fe^{3+} + e^- \rightarrow Fe^{2+} \quad (4)$$

Taking advantage of these benefits, in recent years, extensive research has been conducted on the degradation of organic pollutants in wastewater using electro-Fenton processes. Although the electro-Fenton technology plays a crucial role in treating organic compounds in wastewater, it also has significant drawbacks. Specifically, due to the easy coagulation of Fe^{2+} under alkaline conditions, the electro-Fenton process is limited by the pH (optimal at around pH 3) and the inherent drawbacks of iron sludge.[22]

To address the issues associated with the electro-Fenton reaction, it is imperative to develop metal-free EAOPs capable

of efficiently generating H_2O_2 and enabling in situ activation without requiring additional iron-based catalysts. Fortunately, studies have demonstrated that carbon-based materials can serve as highly effective catalysts for activating H_2O_2 to produce •OH.[23] Therefore, the development of metal-free carbon catalysts presents a promising solution to circumvent the inherent limitations of conventional electro-Fenton systems. Specifically, first, O_2 introduced into the solution receives two electrons at the cathode to generate H_2O_2, as shown in Equation (5).[24] Subsequently, H_2O_2 undergoes catalytic activation by catalytic sites of carbon materials, yielding hydroxyl radicals (•OH). These radicals then react with residual H_2O_2 to generate the superoxide radical ($•O_2^-$), as shown in Equation (6–8).[24] Besides, the generated $•O_2^-$ reacts with H_2O_2 or •OH to form $^1O_2$, as shown in Equation (9) and (10).[24] The production of $^1O_2$ is also accompanied by the reaction of $•O_2^-$ with H_2O or the self-recombination of $•O_2^-$ with H^+,[24] as shown in Equation (11) and (12).

$$O_2(g) + 2H^+ + 2e^- \rightarrow H_2O_2 \quad (5)$$

$$H_2O_2 + e^- \rightarrow OH^- + •OH \quad (6)$$

$$H_2O_2 + •OH \rightarrow H_2O + OOH• \quad (7)$$

$$OOH• \rightleftharpoons H^+ + •O_2^- \quad (8)$$

$$•O_2^- + H_2O_2 \rightarrow OH^- + •OH + {}^1O_2 \quad (9)$$

$$•O_2^- + •OH \rightarrow OH^- + {}^1O_2 \quad (10)$$

$$2•O_2^- + 2H_2O \rightarrow {}^1O_2 + H_2O_2 + 2OH^- \quad (11)$$

$$2•O_2^- + 2H^+ \rightarrow {}^1O_2 + H_2O_2 \quad (12)$$

$$•OH + OOH• \rightarrow O_2 + H_2O \quad (13)$$

$$•OH + •O_2^- \rightarrow O_2 + OH^- \quad (14)$$

Nevertheless, when an excess of active species is generated on the catalyst, •OH and $•O_2^-$ are likely to combine and self-annihilate, as described in Equation (13) and (14),[24] leading to a reduction in pollutant degradation. Because of the synergistic effect of radicals (•OH and $•O_2^-$) and nonradicals ($^1O_2$), the catalyst demonstrates exceptional catalytic performance across a broad pH range of 3–11.

Compared to •OH, $^1O_2$ exhibits considerably greater stability across a broader pH spectrum, rendering it more versatile in diverse aqueous environments. Its lifetime in water (≈2–4 μs)[25] is significantly longer than that of •OH (≈10^{-3} μs),[26] allowing for more extended interaction with target contaminants. Additionally, as a metastable species possessing vacant π* orbitals, $^1O_2$ displays selective oxidative reactivity, preferentially targeting electron-rich organic compounds.[27]

2.2. Peroxymonosulfate-Based EAOPs

Recently, there has been a surge of interest in research focusing on the electro-activation of PMS, which is an inorganic peroxide compound for wastewater treatment.[9,28] This is because compared to •OH, which is the dominant ROS in H_2O_2-based EAOP, $SO_4•^-$ exhibits higher reduction potential [$SO_4•^-$ at 2.5–3.1 V, •OH at 1.9–2.7 V vs. standard hydrogen electrode (SHE)], possess a longer half-life ($t_{1/2}$ for $SO_4•^-$ at 30–40 μs, while •OH is ≈10^{-3} μs), and demonstrate broader pH adaptability.[26] Through EAOPs, PMS can be activated to generate $SO_4•^-$ and •OH that can be utilized for wastewater degradation. First, HSO_5^- can be activated via electron transfer through two distinct pathways to generate either $SO_4•^-$ or •OH (Equation (15) and (16)).[29] Subsequently, the produced $SO_4•^-$ can further react with water molecules to form •OH (Equation (17)).[29] Finally, HSO_5^- can also react with SO_5^{2-} through two different pathways to produce a nonradical species, $^1O_2$, which also plays a significant role in the degradation of organic pollutants in aqueous solution (Equation (18) and (19)).[29,30]

$$HSO_5^- + e^- \rightarrow SO_4^{2-} + •OH \quad (15)$$

$$HSO_5^- + e^- \rightarrow OH^- + SO_4•^- \quad (16)$$

$$SO_4•^- + H_2O \rightarrow HSO_4^- + •OH \quad (17)$$

$$HSO_5^- + SO_5^{2-} \rightarrow HSO_4^- + SO_4^{2-} + {}^1O_2 \quad (18)$$

$$HSO_5^- + SO_5^{2-} + •OH + e^- \rightarrow 2SO_4^{2-} + H_2O + {}^1O_2 \quad (19)$$

2.3. Peroxydisulfate-Based EAOPs

Research has demonstrated that PDS plays a crucial role in EAOPs for wastewater treatment. This is primarily because PDS can be activated to generate reactive species and exhibits high efficiency in oxidizing organic compounds present in wastewater. Specifically, the electrochemically activated PDS molecule may directly oxidize the adsorbed water molecule to generate •OH, as shown in Equation (20).[31]

$$S_2O_8^{2-} + 2H_2O \rightarrow 2•OH + 2SO_4^{2-} + 2H^+ \quad (20)$$

Additionally, a few studies also stated the •OH assisted electrochemical activation of $S_2O_8^{2-}$ forming $SO_4•^-$ as mentioned in Equation (21).[32]

$$2S_2O_8^{2-} + 2•OH \rightarrow 2SO_4•^- + 2HSO_4^- + O_2 \quad (21)$$

$S_2O_8^{2-}$ molecules can also be electrochemically reduced at the cathode, resulting in the generation of $SO_4•^-$, as shown in Equation (22).[32]

$$S_2O_8^{2-} + e^- \rightarrow SO_4^{2-} + SO_4•^- \quad (22)$$

Several studies have also indicated that $S_2O_8^{2-}$ can be directly converted into $SO_4•^-$, as shown in Equation (23).[32]

$$S_2O_8^{2-} \rightarrow 2SO_4^{\bullet -} \quad (23)$$

In the application of PDS in EAOPs, $S_2O_8^{2-}$ can be generated through the reaction between SO_4^{2-} and free •OH in the solution (Equation (24) and (25)).[16] The •OH radicals are produced via the anodic oxidation of water (Equation (1)).

$$SO_4^{2-} + {\bullet}OH \rightarrow 2SO_4^{\bullet -} + OH^- \quad (24)$$

$$SO_4^{2-} + SO_4^{\bullet -} \rightarrow S_2O_8^{2-} + e^- \quad (25)$$

Additionally, PDS is also formed through the electrochemical oxidation of sulfate species, as illustrated in Equation (26)[16]

$$2SO_4^{2-} \rightarrow S_2O_8^{2-} + 2e^- \quad (26)$$

Lastly, in the carbon/PDS system, the active sites of carbon materials convert the stable PDS molecule into its activated state [e.g., activated PDS (PDS*)], which has high reactivity toward specific organic compounds.[31] As shown in Equation (27)

$$\text{Carbon} + \text{PDS} \rightarrow \text{Carbon}(\text{PDS}^*) \quad (27)$$

Owing to the numerous advantages of persulfate, researchers have employed sulfate radicals generated through its electrochemical activation to degrade various organic pollutants in wastewater.[33,34]

3. Design and Engineering of Carbon-Based Materials to Enhance the Degradation Rate of Organic Pollutants via EAOPs

Carbon-based materials are widely reported as environmentally friendly catalysts suitable for use in EAOPs. In this section, we present a summary of the most recent developments in the fabrication and modification of carbon-based materials.

3.1. Carbon-Based Materials and their Composites used in the Processes Involve Activating H_2O_2

3.1.1. Carbon-Based Materials used as Catalysts for Electro-Fenton Reaction

In EAOPs, the electro-Fenton process involves the in situ production and activation of H_2O_2, offering an attractive solution for degrading organic pollutants in wastewater. It is considered sustainable, cost-effective, versatile, and easy to operate. As previously stated, the electro-Fenton reaction, which involves the reaction of Fe^{2+} with H_2O_2 to generate •OH, represents a highly effective approach for the production of •OH within electrocatalytic systems. In this process, H_2O_2 is synthesized in situ via the two-electron ORR, while Fe^{2+} undergoes simultaneous regeneration at the cathode[35] (**Figure 1**a). Therefore, modification of the electrode materials of cathode is crucial for improving the efficiency of the electro-Fenton process in EAOPs.[36]

Various carbon-based materials have been developed for the electro-Fenton oxidation of organic compounds in wastewater, including carbon felts,[37] carbon sponges,[38] carbon cloths (CC),[39] carbon fibers,[40] etc. These materials are favored because of their low cost, excellent conductivity, and high selectivity toward H_2O_2 in the ORR. Among them, carbon foam is a unique porous material with an open-cell structure and a large internal surface area. Given their distinctive structural properties, especially low density and high porosity, these materials represent promising candidates for catalyzing two-electron ORR, generating H_2O_2 as a product. Such properties render them well-suited for application as catalysts in electro-Fenton processes.

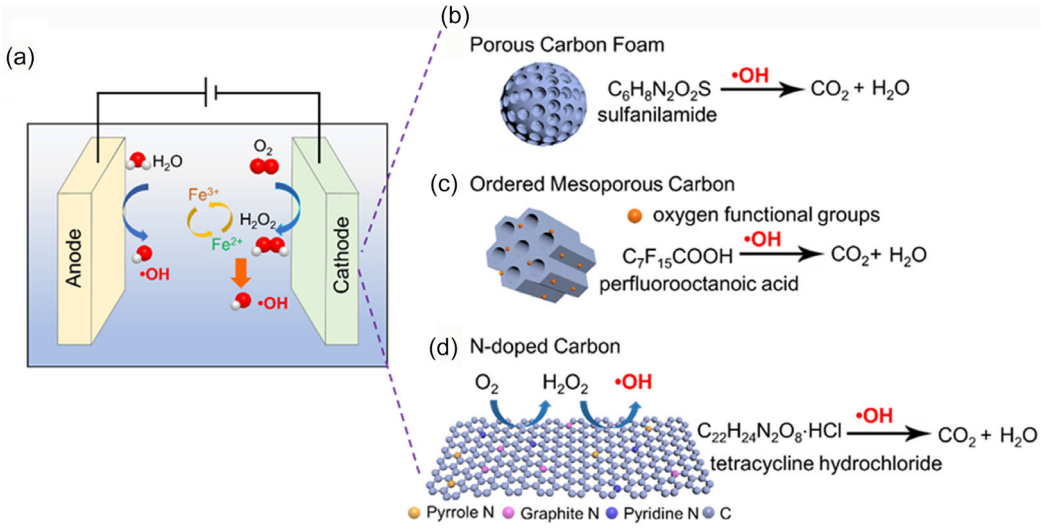

Figure 1. a) Schematic illustration of the electrochemical electro-Fenton process in EAOP. Reproduced with permission.[35] Copyright 2021, Elsevier. b) Schematic representation of sulfanilamide oxidative degradation in the electro-Fenton system using porous carbon foam. Reproduced with permission.[42] Copyright 2021, Elsevier. c) Schematic diagram demonstrating the degradation of perfluorooctanoic acid in the electro-Fenton reaction using ordered mesoporous carbon with oxygen functional groups and nanoconfinement effects. Reproduced with permission.[44] Copyright 2023, Elsevier. d) Schematic illustration of tetracycline oxidative degradation in the electro-Fenton system using NPC. Reproduced with permission.[46] Copyright 2024, Elsevier.

Ganiyu et al. utilized sucrose as a carbon source and employed a polymerization-blowing-carbonization technique to fabricate carbon foam materials, which can be used as a catalyst to facilitate H_2O_2 generation in the electro-Fenton process (Figure 1b).[41,42] The carbon foam produced features a highly porous and extremely lightweight structure, marked by interconnected spherical pores. It exhibits outstanding electrocatalytic performance, including relatively high redox currents and high selectivity to H_2O_2. When employing the carbon foam as a cathode in the electro-Fenton process, complete degradation of 0.5 mM synthetic sulfanilamide solution can be achieved within 4 h. And the electrode exhibits remarkable stability and excellent reusability.

In addition to the inherently large surface area and high electrical conductivity of carbon-based materials, which significantly enhance the electrochemical reaction efficiency, attention must also be given to the unique functional groups on the carbon surface. Previous research has demonstrated that reduced graphene oxide (GO) functionalized with 4-phenoxyphenol with C–O–C bridges is effective in promoting the generation of •OH in electro-Fenton-like reactions.[43] In addition, Tan et al. developed a dual-functional electrocatalyst for the electro-Fenton process, utilizing ordered mesoporous carbons (OMC) endowed with oxygen functional groups as catalysts to effectively produce H_2O_2 and •OH in the electro-Fenton process (Figure 1c).[44] This design was targeted at the degradation of perfluorooctanoic acid in wastewater. Experimental results demonstrated that after 3 h of reaction time, the total organic carbon (TOC) removal rate can be up to 84.0% and the kinetic constant can be 1.26 h^{-1}. The generation of •OH is facilitated by the presence of abundant oxygen functional groups, such as C–O–C, and the nanoconfinement effect provided by the mesoporous channels in the OMC. However, research on the activation of H_2O_2 and production of •OH by oxygen functional groups on carbon materials in the electro-Fenton process remains limited.

In addition to oxygen functional groups, nitrogen doping or nitrogen-containing functional groups can also significantly modify the catalytic property of carbon-based materials in the electro-Fenton process.[45] Specifically, pyridinic nitrogen enhances the Lewis basicity of adjacent carbon atoms, thereby promoting oxygen adsorption. Moreover, the effective protonation of pyridinic nitrogen reduces its ability to cleave the O—O bond, thereby increasing the selectivity of the two-electron ORR. Subsequently, adsorbed oxygen transforms to the *OOH intermediate, which is essential for the formation of H_2O_2.[46] Yu et al. utilized zeolitic imidazolate framework-8 (ZIF-8) as a precursor to developing nitrogen-doped porous carbon (NPC), which was used as a cathode material for removing organic pollutants from the wastewater via the electro-Fenton process.[45] At an initial pH of 7, the application of a modified cathode at 12.5 mA cm^{-2} resulted in a maximum H_2O_2 production rate of 0.74 mg h^{-1} cm^{-2}. Under the same conditions, the graphite electrode without NPC achieved only 0.067 mg h^{-1} cm^{-2}, indicating a 10-fold enhancement in H_2O_2 production with the presence of NPC materials. Furthermore, the NPC-modified cathode effectively removed phenol (50 mg L^{-1}), achieving complete mineralization and a TOC removal efficiency of 82.61% under optimized conditions within 120 min. Additionally, Zhao et al. also developed an NPC from ZIF-8.[46] The difference is that the ZIF-8 was grown on balsa wood and was pyrolyzed together with wood substrate to produce the wood-derived nitrogen-doped porous carbon (WNPC), which served as an electro-Fenton cathode catalyst (Figure 1d). The WNPC exhibited high catalytic selectivity (96%) toward H_2O_2 in the ORR due to the oxygen functional groups and rich nitrogen doping. Moreover, the H_2O_2 production rate of WNPC is three times that of the barberry-derived carbon in the electro-Fenton process. In an electro-Fenton system using WNPC as cathode material, the efficiency for removing tetracycline in wastewater reaches 91% within 120 min, significantly higher than the removal efficiency (63%) using wood-derived carbon as cathode material. This study demonstrated the potential of the electro-Fenton system for eliminating antibiotics in wastewater, either from pharmaceutical factories or animal breeding plants.

Several studies suggest that pyridinic-N is considered a key factor in facilitating two-electron ORR, as the effective protonation of pyridinic-N reduces the capacity to cleave the O—O bond, leading to the favored formation of H_2O_2.[47] Nevertheless, Zhu et al. argue that pyrrolic-N may be more effective in enhancing two-electron ORR.[48] At present, there is no consensus regarding the influence of various forms of nitrogen doping on the two-electron ORR. Current experimental methods are inadequate for creating carbon-based materials with just one type of nitrogen dopant, which makes it challenging to identify the mechanism experimentally. Besides the catalytic activity and selectivity for facilitating two-electron ORR, the adsorption capability for organic pollutants is also critical for the overall efficiency of the electro-Fenton process. Nitrogen doping has been reported to enhance the adsorption characteristics.[49] According to the literature, different forms of nitrogen doping have distinct effects on two-electron ORR performance and lead to differential organic compound adsorption capacities. Thus, the rational design of the type of nitrogen atom and the proportion of nitrogen doping is essential for synergistically enhancing both two-electron ORR performance and organic compound adsorption capacity. To tackle the issue and clarify the synergistic mechanism between two-electron ORR and organic compound adsorption capacity, computational chemistry methods were employed as an effective approach. Unconstrained by external experimental conditions, this method enables precise simulation of a single nitrogen-doped carbon plane for mechanistic investigation. Zhao et al. employed a multiscale simulation approach that combines molecular dynamics and quantum chemistry simulations.[49] Simulation findings indicate that pyridinic-N and pyrrolic-N exhibit synergistic effects, enhancing the tetracycline adsorption ability of activated carbon. Graphitic nitrogen and pyridinic nitrogen significantly improve the selectivity of two-electron ORR, favoring the generation of H_2O_2. Experimental studies suggest a synergistic relationship between organic compound adsorption and two-electron ORR, where a suboptimal performance in either process limits the degradation efficiency of the electro-Fenton process. Proper proportions of pyridinic nitrogen, pyrrolic nitrogen, and graphitic

nitrogen can enhance the synergistic effects of cathode materials between adsorption and two-electron ORR.

The key features of carbon-based materials that affect the performance of electro-Fenton reactions can be summarized into two aspects: pore structure and surface structure. First, Ganiyu et al. developed carbon foam materials with a highly porous and extremely lightweight structure that demonstrated excellent degradation efficiency for sulfanilamide in electro-Fenton systems.[42] In addition to the inherent porous structure of carbon materials, surface modifications—such as oxygen functionalization and heteroatom incorporation—were applied to enhance their degradation efficiency for pollutants in wastewater. Tan et al. fabricated ordered mesoporous carbon catalysts with oxygen-containing functional groups, which showed remarkable removal capability for perfluorooctanoic acid (PFOA) in aqueous solutions.[44] Finally, Yu et al. synthesized nitrogen-doped mesoporous carbon as an EAOP catalyst, with results revealing outstanding catalytic activity for phenol degradation in wastewater.[45]

To enhance the organic pollutant removal efficiency of carbon-based materials in the electro-Fenton process, researchers utilized carbon as a substrate, combining it with metal nanoclusters to achieve performance breakthroughs. Recently, Liu et al. introduced a novel approach involving the use of gold nanocluster-functionalized carbon nanotube filters as electro-Fenton catalysts for decomposing tetracycline in wastewater.[50] Furthermore, Pan et al. employed copper-doped modified graphitic carbon nitride ($g\text{-}C_3N_4$) for the degradation of amoxicillin in wastewater.[35]

Compared to single-metal catalysts, the effective combination of two different metals as bimetallic nanoparticles has been shown to improve catalytic performance through synergistic effects, for instance, the combination of lattice strain and ligand effect.[51,52] Ye et al. reported a simple electrodeposition strategy for preparing bimetallic CuAu catalysts on a CC substrate (**Figure 2**a).[53] The obtained CuAu/CC material can be directly employed as a working electrode, exhibiting outstanding catalytic activity and stability in the electro-Fenton process aiming at the removal of bisphenol A in wastewater. Notably, the bisphenol A removal efficiency can be modified by changing the molar ratio of Cu to Au.

For carbon-based catalysts containing metal content, SACs have also attracted widespread attention because of their distinct tunable electronic structure and maximized metal atom utilization. SACs promote the terminal chemical adsorption of O_2, enhancing the selectivity for two-electron ORR over the four-electron ORR.[54] Various transition metals, including Fe, Ni, and Co, have been used as the active sites in SACs, which have been investigated for two-electron ORR.[41] Both experimental and theoretical studies have shown that Co exhibits the optimal binding energy for *OOH formation, making it a promising candidate for efficient H_2O_2 generation.[41] Yang et al. constructed a nanotube reactor using a spatially isolated and dopant anchoring strategy, where Co-SACs were confined within boron and nitrogen codoped defective carbon nanotubes (Co-B and N-CNTs) to enhance catalytic activity and selectivity for H_2O_2 electrosynthesis through the two-electron pathway.[55] Specifically, the incorporation of boron atoms in the electron-deficient state can alter the electronic distribution around the $Co\text{–}N_x\text{–}C$ sites, improving the binding energy with the *OOH intermediate, and thereby promoting H_2O_2 generation. Furthermore, Zhang et al. developed a $Co\text{–}N_5\text{–}O\text{–}C$ catalyst featuring highly coordinated $Co\text{-}N_5$ moieties and adjacent electron-withdrawing epoxy groups to achieve optimal binding energy for the *OOH intermediate, leading to exceptional mass activity of 87.5 A g^{-1} at 0.75 V versus reversible hydrogen electrode (RHE).[56] This effective in situ production of H_2O_2 further enabled the complete degradation of organic pollutants (methylene blue) within 15 min via the electro-Fenton process (Figure 2b).

3.1.2. Carbon-Based Materials used as Catalysts for Heterogeneous Electro-Fenton Reaction

It is well-known that conventional electro-Fenton processes generally require the addition of Fe^{2+} and the maintenance of an acidic medium to achieve effective pollutant removal. However, pH adjustment may be impractical or economically unfeasible. Consequently, for decades, extensive investigations have focused on broadening the optimal pH range and minimizing metal

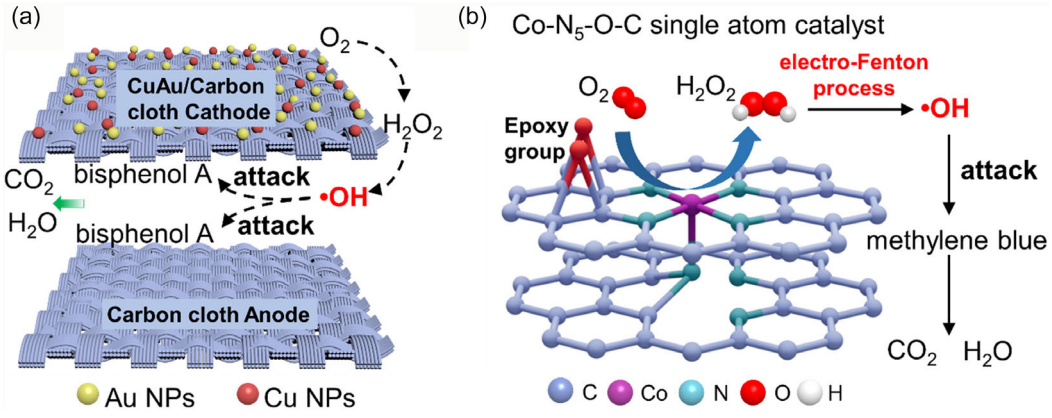

Figure 2. a) Schematic illustration of bisphenol A degradation in the electro-Fenton system using CuAu bimetallic nanoparticles supported on CC. Reproduced with permission.[53] Copyright 2023, Elsevier. b) Schematic representation of methylene blue degradation in the electro-Fenton system utilizing $Co\text{–}N_5\text{–}O\text{–}C$ catalyst. Reproduced with permission.[56] Copyright 2023, Elsevier.

catalyst leaching through the development of innovative heterogeneous electro-Fenton catalysts, with Fe-based catalysts being particularly prominent.[57] These initiatives seek to improve the practicality of electro-Fenton technology, making it more adaptable for diverse wastewater treatment applications. Specifically, the Fe-containing catalytic materials are immobilized on carbon support to substitute dissolved Fe^{2+} as the electro-Fenton reagent, thereby expanding the applicable pH range of electro-Fenton reactions and facilitating a process with easy catalyst recovery. However, while surface-bound Fe(II) efficiently catalyzes H_2O_2 to generate •OH, the kinetics of Fe(III) reduction to regenerate Fe(II) are relatively sluggish, leading to a low •OH production rate and significantly suppressed overall efficiency of the heterogeneous electro-Fenton process. Fortunately, the interaction at the interface between FeO_x nanoparticles and conductive porous carbon supports can improve electron transfer and facilitate the reduction of Fe^{3+}.[58] Furthermore, optimizing the electronic properties of the carbon support through nitrogen doping can further enhance these interface interactions.[59] Cao et al. devised an efficient catalyst featuring FeO_x nanoparticles integrated into nitrogen-doped hierarchical porous carbon (FeO_x/NHPC) (**Figure 3**a).[58] By adjusting the form and content of nitrogen doping, they enhanced the selectivity and generation rate of H_2O_2. The resulting FeO_x/NHPC750 exhibited excellent catalytic activity for H_2O_2 production, showing a low overpotential of 190 mV and H_2O_2 selectivity ranging from 95% to 98% within the voltage interval of −0.3 to −0.8 V. The robust interface interactions between FeO_x and NPC support bolstered the regeneration of Fe(II), leading to the rapid decomposition of H_2O_2 into •OH.

In addition to focusing on the catalytic efficiency of heterogeneous electro-Fenton cathodic catalysts, we should also pay attention to and enhance the catalyst's stability under adverse conditions during the electro-Fenton process. The spatial confinement effect of the outer shell and pore structure can inhibit the aggregation and dissolution loss of the encapsulated active Fe species during the catalytic reaction, resulting in enhanced electrocatalytic activity and excellent stability.[60,61] Significantly, the efficient electron transfer between the carbon shell and the active Fe core may enhance the catalytic performance.[62] For this purpose, significant efforts have been dedicated to synthesizing various electro-Fenton catalysts with core/shell structures. Additionally, Cao et al. synthesized FeO_x/CuN_xHPC by incorporating Cu into the iron-based metal-organic frameworks (MOFs) [NH_2-MIL-88B(Fe)] and subsequently carbonizing the material.[63] The synthesized catalyst exhibited outstanding electro-Fenton activity and stability. Furthermore, extensive research indicates that heteroatom doping, like N, O, and S, can modulate the electronic structure of carbon atoms to generate efficient active sites, thus enhancing the ratio of two-electron ORR.[64,65] Therefore, Zhang et al. used Fe^{3+}-loaded poly(imine dioxime) film as a precursor and successfully prepared iron-based nanoparticles incorporated within NPC (Fe/Fe_3C@NPC) as a cathodic catalyst for the heterogeneous electro-Fenton degradation of bisphenol A (Figure 3b).[66] Within 120 min, the catalyst achieved nearly 100% bisphenol A removal efficiency and 69.2% removal efficiency of the TOC content. In addition, the developed composite catalyst demonstrates exceptional performance in terms of reusability and stability. After six consecutive degradation tests, it

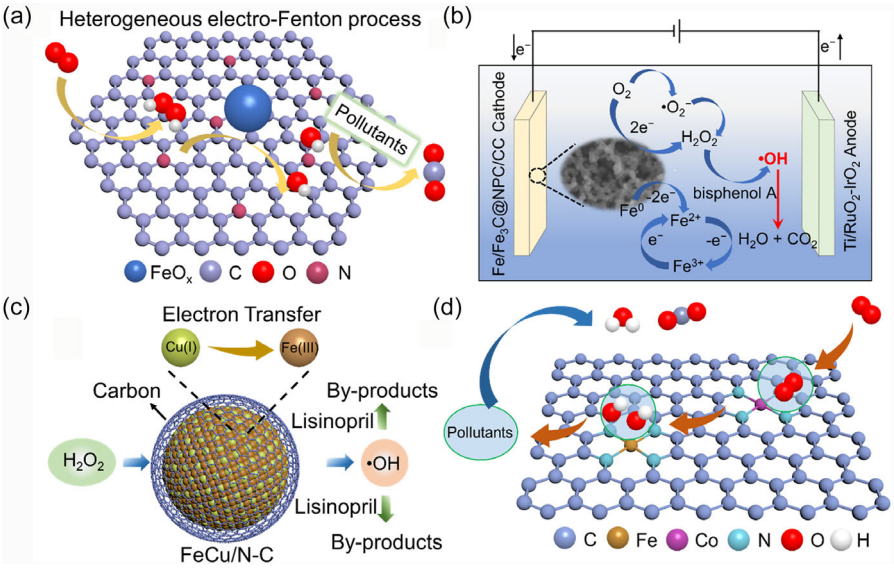

Figure 3. a) Schematic illustration of aqueous pollutant degradation in a heterogeneous electro-Fenton system using FeO_x nanoparticles incorporated in nitrogen-doped hierarchical porous carbon. Reproduced with permission.[58] Copyright 2020, Elsevier. b) Schematic representation of bisphenol A degradation in aqueous solution using a core-shell-structured catalyst composed of Fe nanoparticles incorporated in NPC material, applied in a heterogeneous electro-Fenton. Reproduced with permission.[66] Copyright 2023, Elsevier. c) Schematic diagram demonstrating the degradation of Lisinopril in aqueous solution using carbon-encapsulated bimetallic FeCu nanoparticles. Reproduced with permission.[67] Copyright 2024, Elsevier. d) Schematic illustration of phenol degradation in aqueous solution employing a bimetallic FeCo single-atom catalyst supported on nitrogen-doped carbon material. Reproduced with permission.[77] Copyright 2023, American Chemical Society.

exhibits only a slight decrease in removal efficiency, accompanied by minimal iron leaching (<0.5 mg L^{-1}).

Furthermore, studies have demonstrated that the carbon layers derived from the pyrolysis of MOFs can serve as protective barriers to mitigate metal leaching. Simultaneously, these carbon layers facilitate the regeneration of Fe(II) by reducing the reduction overpotential of Fe(III).[67] To date, several MOFs have been successfully employed as catalysts in EAOPs.[68,69] However, the slow formation of Fe(II) represents a significant bottleneck in the heterogeneous electro-Fenton reaction.[70] To address this issue, researchers have proposed the strategy of employing bimetallic nanocatalysts. Copper has been identified as a promising candidate for this approach,[71] as the standard reduction potential of Cu^{2+}/Cu^{+} (0.17 V) is lower than that of Fe^{3+}/Fe^{2+} (0.77 V), making the reduction of Fe^{3+} by Cu^{+} thermodynamically favorable.[72] Therefore, Zhao et al. successfully synthesized a carbon-encapsulated bimetallic structure (denoted as FeCu/NC) and applied it in a heterogeneous electro-Fenton reaction for the treatment of 16.1 mg L^{-1} antihypertensive lisinopril solution (Figure 3c).[67] At pH 3, complete degradation occurred in 6 min with only 0.05 g L^{-1} of FeCu/NC. Moreover, under near-neutral pH conditions, 100% removal was possible in real municipal wastewater, taking 60 to 75 min. The FeCu/NC catalyst demonstrated excellent stability, retaining 86.5% removal efficiency after five cycles and showing minimal iron leaching. Consequently, the FeCu/NC-based heterogeneous electro-Fenton catalyst demonstrates significant potential for further application in wastewater treatment.

Regarding stability, the aggregation of catalysts is a critical challenge, particularly for materials containing magnetic iron content such as Fe_3O_4 and Fe^0. This phenomenon significantly reduces their active surface area and metal utilization efficiency, thus impairing the removal effectiveness of organic pollutants in heterogeneous electro-Fenton systems.[13,73] Recently, SACs featuring atomically dispersed metal active sites have garnered considerable interest in EAOPs.[74,75] Owing to their maximized exposure to active sites and strong metal-support interactions, SACs demonstrate greater catalytic activity and stability than traditional nanoparticle-based catalysts.[75] Guo et al. synthesized a novel heterogeneous electro-Fenton catalyst, denoted as Fe-N/C, using an iron-doped zeolitic imidazolate framework as the precursor.[76] The optimized 0.3Fe-N/C catalyst demonstrated exceptional catalytic activity for removing carbamazepine over a broad pH range of 3–11, with remarkably low iron leaching (less than 0.3 mg L^{-1} even at pH 3). Moreover, the 0.3Fe-N/C catalyst demonstrated outstanding durability over seven consecutive cycles and showcased broad applicability for degrading various pollutants. To enhance the catalytic efficiency of SACs in heterogeneous electro-Fenton processes, tailoring dual-active-site SACs specifically for H_2O_2 generation and H_2O_2 activation represents a viable approach to address this challenge. This approach leverages the synergistic effects of dual-active sites to optimize both the generation and activation of H_2O_2, thereby significantly improving the overall catalytic performance. Qin et al. have developed a CoFe dual-atom-catalyst (CoFe DAC) designed for synergistic catalysis in the generation of H_2O_2 and •OH (Figure 3d).[77] In this catalyst, dispersed individual Co sites are utilized to enhance H_2O_2 selectivity, while dispersed Fe sites work toward increasing the yield of •OH by activating the generated H_2O_2. In the heterogeneous electro-Fenton process, CoFe DAC demonstrates complete phenol removal, showcasing outstanding stability and low energy consumption, surpassing Fe NC (77.1%), Co NC (66.5%), and NC (51.5%) systems. This study clearly illustrates the continuous production of •OH in the electro-Fenton process mediated by dual-active sites, enhancing the efficiency of organic pollutant removal.

3.1.3. Carbon-Based Materials for Nonelectrochemical Fenton Reaction

Although various modifications and improvements have been made to address the challenges associated with the electro-Fenton reaction, including the development of heterogeneous electro-Fenton catalysts using carbon-based materials with Fe content,[78] only a limited number of these catalysts exhibit satisfactory catalytic performance under neutral pH conditions.[79] Moreover, issues such as Fe-based nanoparticle detachment, agglomeration, and dissolution, which result in a decline in catalytic activity, are also encountered during wastewater treatment processes.[80] To avoid the above issues, researchers developed a system in which conventional electrochemical Fenton reagents (e.g., Fe) are not employed to activate H_2O_2 for the generation of reactive radicals and nonradical species.[24] This approach is herein referred to as the nonelectrochemical Fenton reaction, which typically employs metal-free carbon-based catalysts for in situ H_2O_2 production via the two-electron ORR[81] and the subsequent catalytic decomposition of H_2O_2 to produce •OH.[23,82,83] Furthermore, carbon-based materials are nontoxic and exhibit relatively high stability, good electrical conductivity, and a high overpotential for the hydrogen evolution reaction, which is a side reaction.[84] Notably, nitrogen doping is a widely used strategy because it can efficiently modulate the charge distribution of the sp^2 carbon structure, create structural defects, and boost the electron transfer rate.[85] Hence, Su et al. synthesized nitrogen-doped graphene (Nx-GE) through the annealing of melamine and graphene.[86] The experimental findings demonstrated that the incorporation of nitrogen into graphene significantly enhanced the cathode's activity, selectivity, and stability. Furthermore, Yu et al. introduced polyaniline-modified graphite felt (PANI/x-GF) composite cathode prepared via electrodeposition (**Figure 4**a).[22] This electrode facilitates the in situ generation of H_2O_2 via the nitrogen functionalities of doped polyaniline (PANI), which is then activated into •OH. Density functional theory (DFT) calculations and electrochemical tests demonstrated that graphitic N preferentially promotes the two-electron ORR to generate H_2O_2, while pyridinic-N promotes the transformation of H_2O_2 into •OH radicals. The modified cathode demonstrated a remarkable •OH radical conversion efficiency of up to 93%. Consequently, the degradation performance of bisphenol A was significantly enhanced, and the cathode also exhibited excellent catalytic stability.

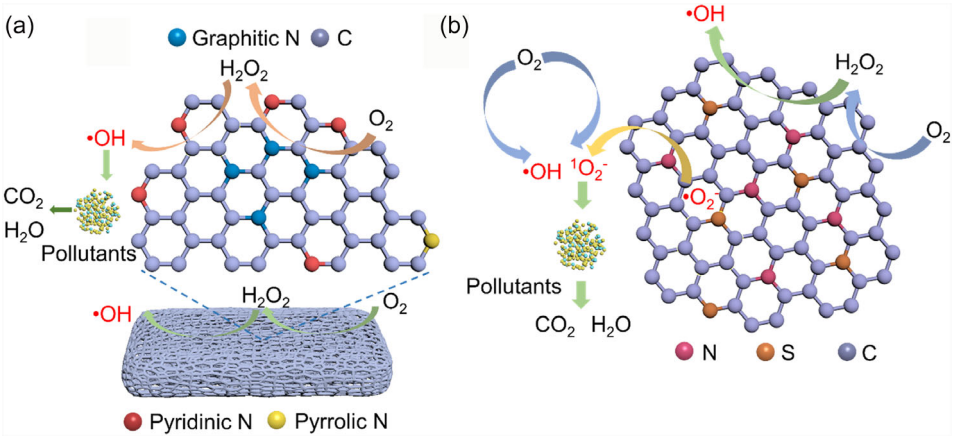

Figure 4. a) Schematic illustration of organic pollutant degradation in aqueous solution using a composite cathode catalyst of nitrogen-doped PANI/x-GF for activating H_2O_2 to generate reactive oxygen species. Reproduced with permission.[22] Copyright 2021, Elsevier. b) Schematic representation of tetracycline degradation in aqueous solution through enhanced reactive oxygen species generation using nitrogen and sulfur self-doped carbon catalyst. Reproduced with permission.[82] Copyright 2025, Elsevier.

Among nonmetal heteroatoms, nitrogen and sulfur are well-known as effective dopants for creating defects in carbon materials.[87] Research has demonstrated that codoping porous carbon with nitrogen and sulfur produces a synergistic effect, significantly enhancing catalytic performance compared to materials doped solely with either nitrogen or sulfur.[82] Therefore, Wang et al. pioneered the synthesis of a bifunctional electrocatalyst from waste ginkgo leaves by adjusting the pyrolysis temperature (Figure 4b).[82] Their research revealed that the self-doping of sulfur and nitrogen in the carbon-based catalysts can synergistically enhance the generation of ROS. At the optimal pyrolysis temperature of 800 °C, the catalyst demonstrated an impressive H_2O_2 selectivity of 94.2% and achieved a tetracycline removal efficiency of 99.3% within 60 min. In situ Fourier-transform infrared spectroscopy (FTIR) and DFT calculations confirmed that graphitic nitrogen serves as the key active site for H_2O_2 production, while pyridinic nitrogen and thiophenic sulfur are the primary active sites for generating •OH radicals. Additionally, nitrogen vacancies were identified as active sites for the production of $^1O_2$ from O_2. The novel cathode exhibited excellent tetracycline degradation performance across a broad pH range (3–11) and maintained exceptional stability over 10 consecutive cycles.

Furthermore, the team pioneered the development of effective in situ metal-free EAOPs based on a flow-through system utilizing waste ginkgo leaf-derived S, N self-doped carbon (SN-BC) catalytic membranes for degrading organic pollutants.[24] The findings demonstrated that organic pollutants were effectively concentrated and catalytically degraded through the in situ generation of reactive species. Compared to traditional electro-Fenton processes, these in situ metal-free EAOPs demonstrated broader pH adaptability and improved efficiency, while simultaneously excluding the formation of iron sludge and the necessity for additional catalysts. Consequently, this approach holds significant promise for the advancement of metal-free EAOPs aimed at environmental restoration.

3.2. Carbon-Based Materials for Activating Peroxydisulfate and Peroxymonosulfate

Compared to activating H_2O_2 to generate •OH, the generation of $SO_4•^-$ through persulfate activation is gaining increasing attention in pollutant removal. This is due to the long-lived radicals produced in this process, the broad pH range, and high selectivity.[88] To attain high yields of $SO_4•^-$, the development of efficient catalysts for persulfate activation is a significant approach. In recent years, the activation of transition metals has attracted greater research interest because of their potential for energy savings, affordability, and high efficiency.[89] Transition metals demonstrate outstanding effectiveness in activating persulfate due to their ability to easily donate electrons, facilitating the cleavage of O—O bonds in PMS. Studies have shown that cobalt is regarded as one of the most efficient transition metals for activating PMS. Presently, Co catalysts have been widely employed to activate PMS for generating reactive species to oxidize organic pollutants in wastewater.[90] However, the performance of unsupported transition metal catalysts is not as remarkable as that of supported transition metal catalysts. It has been noted that cobalt oxide on activated carbon shows outstanding efficacy in persulfate activation, exhibiting greater activity than both unsupported heterogeneous Co_3O_4 catalysts and homogeneous Co^{2+} ions.[91] Research indicates that carbon-based materials are commonly utilized as substrates for metal nanoparticles because of their stability, excellent conductivity, and low cost.[92] Among carbon materials, carbon felt demonstrates superior performance at moderate to low current densities and can serve as a substrate for metal catalysts.[93] The dispersion of cobalt chemically bound to carbon felt minimizes metal leaching, facilitates electron transfer, and improves catalytic activity.[94] Lin et al. prepared nitrogen and cobalt-modified carbon felt (Co-N@CF) to effectively activate PMS for the removal of tetracycline.[95] The Co-N@CF catalyst demonstrated excellent catalytic performance and stability for

PMS activation, achieving a tetracycline removal efficiency of 92.2% within 1 h under optimal conditions.

Research has shown that catalyst materials derived from ZIF-8 hold promise for effectively activating PMS.[96] However, directly modifying CF with ZIF-8 poses challenges, including irregular adhesion, limited attachment sites, and poor stability. On the other hand, indirect modification of carbon felt with cobalt-based materials presents issues with low ion diffusion efficiency toward the electrode surface. Notably, CNTs have emerged as a novel carbon nanomaterial in recent years, frequently utilized as a support due to their high surface area and outstanding conductivity.[97] Furthermore, as CNTs can offer ion diffusion channels and electron transfer pathways, the combination of CNTs with ZIF-8 is expected to exhibit synergistic effects. Therefore, CNTs can not only address the aggregation issues of ZIF-8 but also offer additional nucleation sites for ZIF-8.[98] Xie et al. prepared a Co@ZIF-8/CNT/CF catalyst for PMS activation through a coelectrodeposition method (**Figure 5**a).[99] The findings indicate that the synthesized Co@ZIF-8/CNT/CF catalyst effectively activates PMS for tetracycline removal. In comparison to the bare carbon felt and PMS reaction system, the Co@ZIF-8/CNT/CF-PMS system demonstrated a 67.5% reduction in activation energy and a 4.21-fold enhancement in reaction rate constant, thereby promoting favorable kinetic processes for PMS activation.

Furthermore, iron-based materials are among the most commonly employed catalysts in PMS-based EAOPs due to their excellent catalytic activity toward PMS and their environmental friendliness.[100] Currently, there is growing interest in composite catalysts over iron-based materials, as the combination of iron with other transition metals can significantly boost catalytic activity.[101] Recent studies have shown that iron-manganese oxides exhibit excellent PMS activation capabilities.[102] Xu et al. synthesized manganese-iron oxide/graphite felt (Mn-Fe oxide/GF) cathodes through in-situ reduction and low-temperature calcination (Figure 5b).[103] The prepared Mn-Fe oxide/GF was utilized as a cathode to activate PMS for the degradation of atrazine in EAOP systems. The minimum activation potential of PMS (η_{min}) was measured to evaluate cathode activity, showing that the addition of manganese effectively lowers η_{min} on the iron oxide/GF cathode. Optimized Mn–Fe oxide/GF demonstrated a reduction in energy consumption of about 85.1% in EAOP systems compared to the scenario without manganese. Therefore, this study reduces the minimum activation potential by incorporating Mn and presents an approach for minimizing energy consumption in EAOPs.

Compared with PMS, PDS demonstrates greater potential for degrading organic contaminants due to its lower cost, more convenient storage requirements, and enhanced oxidation efficiency.[104] Recently, metal-free carbon materials have emerged

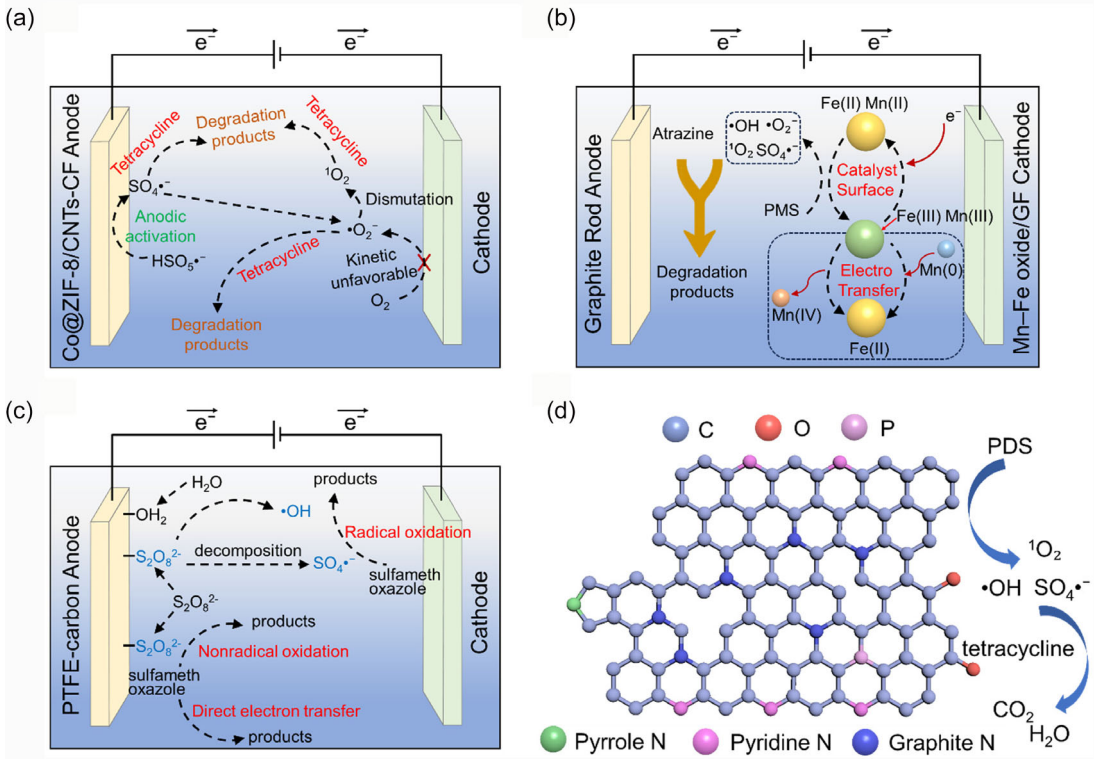

Figure 5. a) Schematic illustration of tetracycline degradation in aqueous solution through electrocatalytic activation of PMS using Co@ZIF-8/CNT/CF catalyst in EAOPs. Reproduced with permission.[99] Copyright 2023, Elsevier. b) Schematic representation of atrazine degradation in aqueous solution via electrocatalytic activation of PMS employing Mn-Fe oxide/GF cathode catalyst in EAOPs. Reproduced with permission.[103] Copyright 2024, Elsevier. c) Schematic representation of sulfamethoxazole degradation in aqueous solution via electrocatalytic activation of PDS employing (PTFE)-modified carbon electrodes in EAOPs. Reproduced with permission.[31] Copyright 2018, Elsevier. d) Schematic representation of tetracycline degradation in aqueous solution via electrocatalytic activation of PDS employing NPCs-35 in EAOPs. Reproduced with permission.[105] Copyright 2023, Elsevier.

as promising alternatives to metal-based catalysts for PDS activation, eliminating the risk of toxic metal ion leaching.[105] Moreover, nonradical oxidation mediated by carbon-activated PDS is minimally affected by water matrices, making it a promising technology for wastewater treatment. Based on the reaction location, electrochemical activation of PDS can be classified into two categories: cathodic activation and anodic activation. SO_4•$^-$ are mainly generated through cathodic activation of PDS at the cathode surface, while nonradical species (e.g., $^1O_2$) are produced via anodic activation of PDS at the anode surface.[106] Compared with cathodic activation, anodic activation of PDS demonstrates superior performance in degrading organic pollutants.[107] Accordingly, Song et al. fabricated polytetrafluoroethylene (PTFE)-modified carbon electrodes using four common carbon materials, including multi-walled carbon nanotubes, graphene, carbon black, and granular activated carbon, for the electrochemical activation of PDS at the anode (Figure 5c).[31] The system generated nonradical species (e.g., $^1O_2$) and radical species (•OH, and SO_4•$^-$) during the electrochemical activation process. The formation of a transition-state PDS structure [e.g., activated PDS (PDS*)] adsorbed on the carbon anodes under applied current is critical to the PDS activation process. Experimental results demonstrated that this process exhibited remarkable tolerance to complex aqueous matrices.

Furthermore, previous studies have demonstrated that heteroatom-doped carbon materials can significantly enhance catalytic activity,[108] as the incorporation of heteroatoms with different atomic radii effectively modulates intrinsic electroactive sites and disrupts the chemical inertness of sp^2-hybridized carbon frameworks.[109] Cheng et al. synthesized nitrogen and phosphorus codoped porous carbons (NPCs) using PANI as a precursor for PDS activation to degrade tetracycline in wastewater (Figure 5d).[105] Experimental results indicate that the optimized synthesized NPCs-35 exhibit the largest specific surface area, the highest density of defect structures, and the greatest graphitic nitrogen content, all of which are beneficial for the activation of PDS. Under optimal conditions (0.3 g L^{-1} catalyst, 0.3 g L^{-1} PDS, initial pH 5.0), NPCs-35 catalyst can remove 90.34% of tetracycline within 60 min. In addition, the initial pH value, inorganic anions (HCO_3^-, SO_4^{2-}, NO_3^-, $H_2PO_4^-$, and Cl^-), and water matrix have little effect on the removal efficiency of tetracycline, indicating that NPCs-35 exhibits strong adaptability to environmental changes in EAOPs.

To sum up, the synthesized carbon-based materials demonstrate excellent capability in activating persulfate (PMS and PDS) to generate reactive oxygen species (•OH, SO_4•$^-$, $^1O_2$, and •O_2^-), which can effectively oxidize and degrade organic pollutants in wastewater.

3.3. Quantitative Comparison and Summary of Carbon-Based Materials in EAOPs

To quantitatively compare the organic compound degradation or removal efficiency when using different carbon-based materials, we have summarized performance metrics (including pollutant removal rate, TOC removal rate, kinetic constants, and electric energy consumption (EEC)) based on comprehensive data analysis, as detailed in **Table 1**. This summary could provide a valuable

Table 1. Summary of material performance indicators in EAOPs.

Materials	Organic pollutants	Removal rate	TOC removal rate	Kinetic constant	The EEC	References
Carbon foam[a)]	Sulfanilamide	100%@1 h	/	0.169 s^{-1}	~81.9 kW h kg^{-1}	[42]
OMC	PFOA	92.3–98.0%@2-3 h	84.0%@3 h	1.26 h^{-1}	8.9 kW h m^{-3}	[44]
NPC	Phenol	100%@2 h	82.61%@2 h	/	137.1 kW h kg^{-1}	[45]
WNPC	TC	91%@2 h	59.2%@4 h	~0.017 min^{-1}	/	[46]
CuAu/CC	BPA	99.5%@2 h	64.2%@2 h	/	/	[53]
Co–N_5–O–C	Methylene Blue	100%@15 min	/	0.375 min^{-1}	/	[56]
Co_1–NCB	Phenol	>95%@5 h	88.6%@5 h	0.832 h^{-1}	/	[170]
FeO_x/NHPC	Phenol	99% @ 2 h	83%@7 h	0.034 min^{-1}	/	[58]
Fe/Fe_3C@NPC	BPA	99.5%@80 min	69.2%@2 h	0.063 min^{-1}	/	[66]
FeCu/NC	Antihypertensive lisinopril	100%@60–75 min	37.1%@2 h, 45.1%@6 h	/	/	[67]
CoFe DAC	Phenol	100%@1.5 h	87.2%@3 h	2814.8 min^{-1} g_{cat}^{-1}	19.0 kW h kg^{-1}	[77]
PANI/x-GF	BPA	>97%@0.5 h	90.7%@2 h	0.116 min^{-1}	/	[22]
WLGC-800	TC	98%@40 min	62%@1 h	0.08 min^{-1}	/	[82]
SN-BC	TC	92.1%@2 h	67.2%@2 h	0.02 min^{-1}	16.8 kW h kg^{-1}	[24]
Co@ZIF-8/CNT/CF	TC	94.31%@1 h	/	0.2608 min^{-1}	/	[99]
Mn-Fe oxide/GF	Atrazine	>95%@0.5 h	/	~0.08 min^{-1}	4.95 kW h kg^{-1}	[103]

[a)]Notes: 1) TOC removal rate: Total Organic Carbon Removal Rate; 2) OMC: ordered mesoporous carbons; 3) NPC: nitrogen-doped porous carbon; 4) WNPC: wood-derived nitrogen-doped porous carbon; 5) PANI/x-GF: polyaniline-modified graphite felt; 6) WLGC-800: waste leaf-derived graphitic carbon at the pyrolysis temperature of 800 °C; 7) SN-BC: S, N self-doped biomass carbon; 8) Mn–Fe oxide/GF: manganese–iron oxide/graphite felt; 9) PFOA: perfluorooctanoic acid; 10) TC: tetracycline; and 11) BPA: bisphenol A. The symbol '~' denotes that the data were extracted from graphs reported in the literature. The EEC data represent energy normalized by the volume of solution or by the mass of organic pollutants (e.g., specific organic compounds, chemical oxygen demand, or TOC) as reported in different studies.

reference for future research on carbon-based materials in application of EAOPs.

Furthermore, carbon-based materials have received extensive attention due to their tunable physical and chemical properties, excellent electrical conductivity, and structural versatility. Through a comprehensive literature review, we identified that the activation efficiency of typical peroxide agents used in EAOPs—H_2O_2, PMS, and PDS—is highly dependent on the structural characteristics of carbon materials, including doping elements, defect densities, and surface functionalities.

For H_2O_2 activation, materials with high electron transfer capability and abundant active sites are preferred. Nitrogen-doped carbon (N–C) materials, such as N-doped graphene,[86] N-doped porous carbon,[46] and N-doped carbon nanotubes,[110] have been shown to effectively facilitate H_2O_2 activation. This is attributed to the presence of pyridinic and graphitic nitrogen, which modulate the electronic distribution within the carbon matrix, thereby enhancing both the generation and decomposition efficiency of H_2O_2. Additionally, defect-rich carbon materials also exhibit promising H_2O_2 activation performance, as the presence of vacancies and edge sites contributes to electron delocalization and improved catalytic activity.[111]

In the case of PMS activation, the cleavage of the O—O bond to generate $SO_4•^-$ and •OH radicals is a critical step. This process is significantly enhanced by introducing surface electronic defects and heteroatom doping. Codoped carbon materials, particularly N, S-codoped carbons, have been extensively reported. Sulfur doping introduces local electronegativity gradients, which promote PMS adsorption, while nitrogen doping facilitates electron transfer kinetics.[112–114] Moreover, graphene-based materials such as GO have been utilized, where oxygen-containing functional groups—especially carboxyl and epoxide groups-serve as active sites for PMS activation.[115]

PDS activation, on the other hand, demands stronger electron-donating capabilities to cleave the symmetric $S_2O_8^{2-}$ structure. Porous carbons, particularly those derived from biomass, have emerged as effective activators due to their high specific surface area, hierarchical porosity, and abundant defect sites, which together promote PDS diffusion and electron transfer.[116] Carbon nanotubes (CNTs) have also shown excellent performance in PDS activation. The curvature of CNT walls induces localized electronic structures that enhance PDS adsorption and activation.[117]

In addition to material–oxidant compatibility, the selection of oxidants must be aligned with the chemical nature of the target pollutants. H_2O_2 predominantly produces nonselective •OH, which are highly reactive toward electron-rich organic pollutants such as phenol, Sulfamethoxazole, and tetracycline. Under alkaline conditions, reactive species such as $•O_2^-$ and $^1O_2$ may also form, expanding the oxidative potential of H_2O_2-based systems. PMS activation, which primarily yields $SO_4•^-$ and •OH, favors the degradation of compounds possessing electron-rich moieties, such as –OH, $–NH_2$, and C═C bonds. It has been successfully applied to degrade tetracycline[95] and bisphenol A.[118] In comparison, PDS activation generates more $SO_4•^-$ radicals and is particularly suitable for breaking strong C—F and C—Cl bonds. This makes PDS highly effective in treating persistent micropollutants such as PFOA, perfluorooctane sulfonate (PFOS), and chlorinated hydrocarbons.[119–121]

Collectively, these findings highlight the necessity of tailoring carbon-based catalysts based on the specific reactivity requirements of peroxides and the structural features of target pollutants. Such a systematic understanding not only facilitates the rational design of redox-active materials but also provides a valuable framework for optimizing EAOP systems in wastewater treatment applications.

To better demonstrate the relationship among carbon-based materials, peroxides, and the degradation of organic pollutants in EAOPs, we created the corresponding table, as shown in **Table 2**.

4. Application of Carbon-Based Materials in EAOPs

4.1. Utilization of Carbon-Based Materials in Bipolar Electrode Systems

Research indicates that carbon-based materials can modulate the transfer of electrons from organic pollutants to peroxides or alter the structure of carbon materials, thereby inducing direct oxidation processes on the material surface.[122] However, compared to metal-based catalysis, the oxidation capacity of carbon-based EAOPs remains significantly limited due to the inherently weak electron transfer capabilities of the material surface.[123] Additionally, carbon-based materials often face deactivation issues, such as depletion of active sites, pore blockage, and accumulation of degradation by-products, leading to a significant decline in catalytic performance.[123] While traditional electrochemical methods have addressed many challenges, as a typical heterogeneous reaction process, they still encounter several common technical hurdles. These include limitations in electrode surface area leading to mass and electron transfer restrictions, as

Table 2. The correlation table of carbon-based materials, peroxides, and degraded organic pollutants in EAOPs.

Carbon materials	Peroxides	Generated reactive oxygen species	Organic pollutants that tend to degrade
Porous carbon materials, Carbon nanotubes	PDS	$SO_4•^-$, •OH, $•O_2^-$, $^1O_2$	Perfluorinated compounds (PFOA, PFOS), Chlorinated hydrocarbons
Nitrogen-doped carbon materials	H_2O_2	•OH, $•O_2^-$, $^1O_2$	Phenol, Sulfamethoxazole, Tetracycline
Co-doped carbon materials	PMS	$SO_4•^-$, •OH, $•O_2^-$, $^1O_2$	Tetracycline, Bisphenol A

well as high energy and chemical consumption due to low current efficiencies and the need for electrolyte support.[124] By investigating the distinct advantages of electrochemical methods and carbon catalysis, researchers have developed effective solutions. Studies have shown that electric fields can propel conductive objects, including carbon-based materials like CNTs and reduced GO, to generate bipolar electrodes through charge separation. According to bipolar electrochemistry, asymmetric redox reactions occur on the two poles of the electrode through charge separation.[125] Carbon-based materials polarize under an external electric field, which can serve as numerous electron donors and acceptors, significantly enhancing electron transfer on the material surface.[126] Consequently, a method utilizing dual-functional bipolar electrodes needs to be designed to address critical issues in EAOPs, such as mass and electron transfer limitations, catalyst deactivation problems, and so on. Ge et al. utilized CNTs as dual-functional bipolar electrodes under an electric field to modulate electron transfer (**Figure 6**).[127] This approach allows CNTs to act simultaneously as electron donors and acceptors to regulate the direct oxidation of organic pollutants. It effectively addresses two significant challenges in EAOPs: mass and electron transfer limitations and catalyst deactivation. In addition, Sun et al. developed an innovative bipolar electrode system employing a graphite electrode modified with graphite/TiO_2 composite.[128] Through systematic analysis grounded in bipolar electrochemical principles, the team elucidated the electrochemical reaction mechanisms, operational parameters, and energy consumption profiles of the system. The optimized configuration demonstrated remarkable performance, achieving •OH generation of 26.813 mg L^{-1} h^{-1} under 2.0 V applied potential within 1 h operational duration. This radical yield corresponds to a 58% enhancement in pseudo-first-order degradation kinetics compared to conventional electrode systems, particularly evident in the mineralization of refractory organic pollutants.

In addition to electrochemical bipolar strategies, multi-field coupling technology has garnered significant attention in catalysis due to its synergistic enhancement effects. Particularly in electrochemical systems, this approach demonstrates not only superior catalytic performance but also excellent environmental compatibility. Consequently, multi-field coupling has been

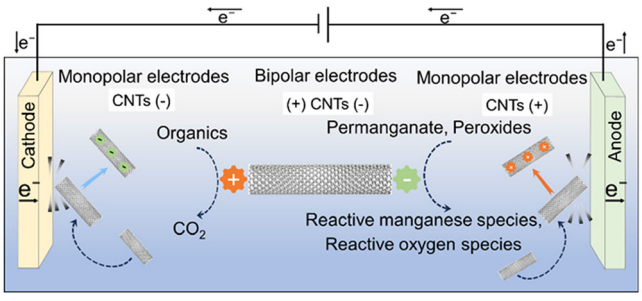

Figure 6. Schematic illustration of electron transfer and PMS activation for reactive radical generation using CNTs as a bifunctional bipolar regulating material under an electric field. Reproduced with permission.[127] Copyright 2024, American Chemical Society.

successfully implemented in EAOPs for effective organic pollutant removal in wastewater.

4.2. External Fields Assisted Degradation of Organic Pollutants Catalyzed by Carbon-Based Materials

Photoelectrochemical catalysis is widely adopted in AOPs.[2,129–131] In the photoelectrochemical process, the combined driving force from photon excitation and electrical potential leads to the accelerated production of reactive radicals, which facilitates the oxidative degradation of organic pollutants. This synergistic effect, resulting from the integration of electrochemical oxidation and photocatalysis, significantly enhances the efficiency of AOPs.[2] Analogous to traditional photocatalysis, photoelectrochemical catalysis predominantly employs semiconductor metal oxides. When irradiated by photons with adequate energy, these materials generate electron–hole pairs that drive catalytic reactions. However, unlike photocatalysis, photoelectrochemical catalysis can mitigate the rapid recombination of these photo-generated electron–hole pairs by applying a bias potential. This bias potential helps to drive the photo-generated electrons away from the semiconductor anode, thereby improving charge separation and enhancing the overall efficiency of the process.[2,132–134] Similar to conventional photocatalysis, semiconductor metal oxides are commonly used in photoelectrochemical catalysis. The main materials include TiO_2,[135,136] $BiVO_4$,[137] MoS_2,[138] Cu_2O,[139] Fe_2O_3,[140] and WO_3.[141] Significantly, carbon materials possess several advantages, including high dimensional stability, large specific surface area, excellent electrical conductivity, and high electrocatalytic activity, while also minimizing electrode surface contamination. These properties make carbon materials highly suitable for integration with metal oxide semiconductor nanoparticles, playing a crucial role in the PEC-based degradation of water pollutants.[142] Therefore, Nada et al. fabricated CZnO-Pd composite material via electrospinning and atomic layer deposition for application as a new photoanode in the photoelectrochemical degradation of paracetamol (**Figure 7**a).[143] Upon utilizing this material in photocatalysis, complete removal of paracetamol was obtained within 3 h under a current density of 10 mA cm^{-2}. The TOC removal rate reached 71.20 ± 0.31% after 4 h, indicating significant mineralization. The findings highlight the substantial potential of Pd–ZnO/C in the photoelectrochemical removal of organic micropollutants. Fan et al. developed a Bi_2WO_6/CA composite electrode where carbon aerogel serves as the adsorbent and Bi_2WO_6 as the photocatalyst, effectively enabling synergistic adsorption and photocatalysis.[144] Under alkaline conditions (pH > 12), applying a potential greater than 0.6 V [vs. saturated calomel electrode (SCE)] resulted in the adsorption of over 90% of nonylphenol, with most of it accumulating on the electrode. Due to the effective adsorption enrichment and the excellent photoelectrochemical performance of the electrode, the nonylphenol accumulated on the electrode was completely degraded during the photocatalytic process (99.3% removal). Benjamin O. Orimolade et al. fabricated a catalyst composed of a graphene-stripped $BiVO_4$/ZnO heterostructure

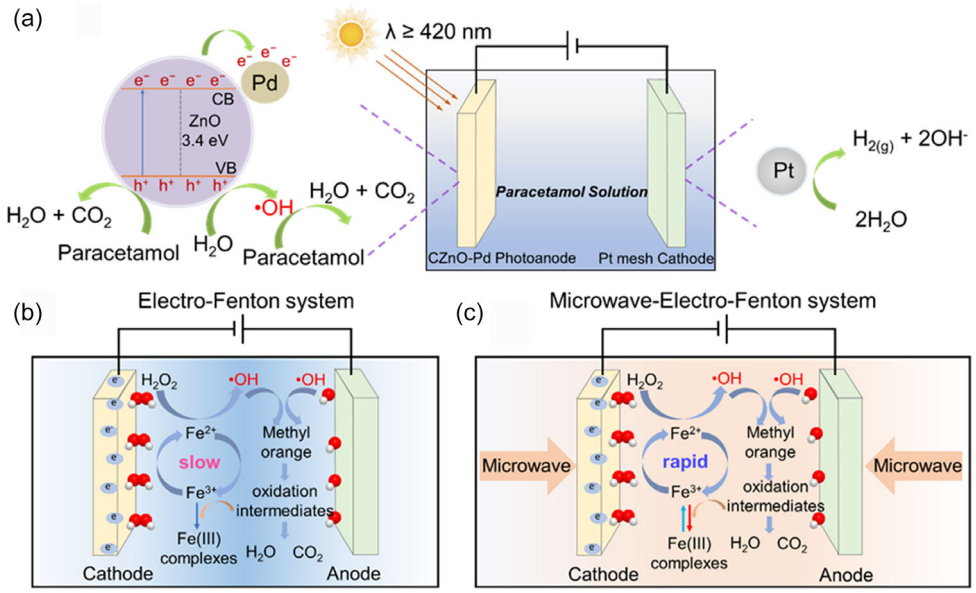

Figure 7. a) Schematic illustration of the photo-electrocatalytic degradation of acetaminophen using CZnO-Pd composite materials. Reproduced with permission.[143] Copyright 2021, Elsevier. Schematic diagram of reaction mechanism in b) electro-Fenton and c) the microwave-assisted electro-Fenton system. Reproduced with permission.[146] Copyright 2012, American Chemical Society.

nanocomposite.[145] Using this composite electrode, applying a current density of 10 mA cm^{-2} in a solution with a pH of 7 resulted in an outstanding degradation efficiency of Rhodamine B, reaching 91%.

Additionally, in EAOPs, a reduction in the efficiency of catalytic degradation reactions may occur due to the adsorption of pollutants and intermediates on the electrode surface, leading to the blockage of active sites.[146] To tackle this challenge, researchers suggest that microwave irradiation can induce localized overheating near the electrode-electrolyte interface, thereby facilitating the electrochemical processes.[147] Wang et al. accelerated the degradation efficiency of pollutants by incorporating microwave irradiation into an electro-Fenton system.[146] Specifically, microwave effectively activates both the cathodic and anodic surfaces. As illustrated in Figure 7b,c, on the cathodic side, microwave introduction not only facilitated O_2 reduction to produce H_2O_2 but also accelerated the Fe^{2+}/Fe^{3+} redox cycle, thereby expediting the electro-Fenton process. On the anodic side, more active sites for •OH generation were created on the electrode surface. Experimental results demonstrate that the formation and degradation rates of intermediates in the microwave-electro-Fenton system were significantly enhanced compared to the setup without microwave assistance due to the synergistic effect between microwave irradiation and the electro-Fenton process. Furthermore, the removal rates of TOC and methyl orange, as well as the mineralization current efficiency, were ≈3.1, 1.1, and 3.2 times higher, respectively, than those without microwave irradiation.

Both the electrochemical bipolar configuration and the multi-field coupling system have demonstrated outstanding treatment capabilities for organic wastewater via EAOPs. Improving device design could also be a promising direction for EAOP research.

4.3. EAOPs Combined with Redox Flow Battery

Flow batteries have emerged as a significant technology for sustainable energy storage and power supply.[148–155] As previously mentioned, carbon-based materials and their composites have played a crucial role in the removal of organic pollutants from wastewater through EAOPs. Therefore, it is theoretically feasible to utilize a gas diffusion electrode composed of carbon-based materials to replace the positive electrode in a flow battery. In this configuration, a two-electron ORR occurs at the positive electrode, catalyzed by the carbon-based materials, generating H_2O_2 as a source of reactive oxygen species for the degradation of pollutants in wastewater. Simultaneously, an electrochemical oxidation reaction occurred at the negative electrode, providing the protons and electrons required at the positive electrode. This type of galvanic cell configuration involves in situ H_2O_2 generation, which has already been demonstrated practically in Zn-air batteries.[156,157] When in operation, this device can simultaneously purify water and generate electricity through electrochemical reactions at both electrodes. As a result, this flow cell system enables the EAOP device to function in outdoor environments without the need for an external power supply.

In this type of device, particular attention should be given to the electroactive chemical species introduced on the anode side. Since the initial development of redox flow batteries, various metal-based active materials have been proposed as electroactive species, including all-vanadium,[158] zinc–cerium,[159] vanadium–cerium,[160] and all-copper systems.[161] Among these, the all-vanadium redox flow battery has been the most extensively studied due to its high reversibility and relatively high power output. However, the high production cost associated with vanadium-based systems has posed a significant barrier to their

widespread commercialization.[162] In contrast, certain organic molecules have emerged as promising alternatives to metal-based active materials in redox flow batteries, due to their low cost and the chemical tunability of organic molecules, which plays a pivotal role in redox flow battery systems.[163] By strategically modifying organic molecules, key electrochemical properties of organic molecules can be precisely tailored, including enhanced solubility, tunable redox potentials, and improved stability, ultimately enhancing battery performance in terms of energy density, power density, and cycle life.[164] Currently, numerous organic molecules—including viologens,[165] alloxazines,[166] and phenazines,[167] have been extensively investigated as redox-active materials for flow battery applications. Notably, when integrating organic molecules with cathodes to assemble redox flow batteries, it is essential to employ electroactive species at the negative electrode with relatively low redox potentials. Molecular engineering strategies, such as introducing electron-donating groups ($-CH_3$ and –OH) to viologen derivatives, can effectively shift the redox potential to more negative values.[168] Such modifications not only enhance the overall cell voltage but also improve the operational stability of the flow battery system.

While theoretically feasible, this flow battery system still faces several critical challenges. First, on the positive electrode side, H_2O_2 activation generates numerous radical and nonradical species, which can adversely affect the membrane separating the positive and negative electrode chambers. Moreover, oxygen crossover from the positive to the negative electrode may significantly interfere with the reduction reactions occurring at the negative electrode. To address these issues, developing a novel exchange membrane with tailored properties is essential, thereby facilitating the integration of EAOP with redox flow batteries. We believe that research into this type of galvanic cell configuration device for EAOP may represent a promising direction for the future development of water purification technology.

5. Conclusion and Prospect

In this perspective, we have summarized the recent research about the carbon-based materials used as the electrode composite for EAOPs. The key mechanisms of EAOPs are introduced, including the activation of H_2O_2, PMS, and PDS to generate active species crucial for the degradation of organic compounds in wastewater. Moreover, various materials engineering strategies and corresponding structure-property relationships are discussed, including morphology selection, surface functional group optimization, elemental doping, etc. The reported materials are categorized according to their preferred application situation, for example, electro-Fenton, heterogeneous electro-Fenton, and nonelectro-Fenton processes. Furthermore, methods aimed at improving the overall efficiency of the EAOP setup have been discussed. For instance, improving the electrode structure by fabricating bipolar electrodes with the designed carbon-based materials, and accelerating EAOPs via coupling an external field (e.g., microwave) with the electrode potential. In addition to exploring carbon-based materials themselves, we propose combining EAOPs with redox flow batteries to develop novel flow cells. This device can effectively treat organic pollutants in wastewater while also generating electricity, which holds practical potential, particularly in outdoor environments. We believe this approach represents an important research direction for the future development of EAOPs.

While carbon-based materials already demonstrate excellent performance in the EAOPs, there are still several aspects that require further attention in the future.

5.1. Material Optimization

During the process of organic compound removal in EAOPs, some pollutants and reaction intermediates may adsorb around the catalyst, leading to the deactivation of active sites and a decrease in catalytic activity. Although some solutions have been reported, such as microwave-assisted catalysis, these approaches significantly increase the cost of industrial applications. Therefore, it is desirable to optimize the structure in the nanometer and micrometer scales (e.g., porosity and surface structure) to increase active site density, promote mass transfer, and enhance catalytic efficiency. Furthermore, during the electrocatalytic degradation of organic compounds—typically carried out at lower pH levels (e.g., in the electro-Fenton reaction), in highly oxidative environments, and at high potentials—carbon-based materials are prone to corrosion or structural deformation (e.g., graphitic layer delamination), leading to reduced electrode lifetime. Additionally, metal catalysts loaded on carbon materials may experience metal leaching, which also leads to the degradation of the electrode. Hence, there is a need to develop corrosion-resistant coatings or more stable carbon-based materials with a wider pH range during application.

5.2. Preparation Process Simplification and Cost Reduction

High-performance carbon materials, such as carbon nanotubes and graphene, are widely utilized materials in research. However, traditional synthesis methods often involve complex processes, such as chemical vapor deposition (CVD), which lead to high costs and limit the potential for large-scale production. Therefore, there is a need to explore low-cost, high-efficiency carbon material synthesis techniques.

Biomass carbonization technology is a promising method that utilizes biomass as a raw material and employs controlled pyrolysis or carbonization processes to facilitate the production of carbon materials. Compared to conventional methods, biomass carbonization technology presents several distinct advantages, such as the widespread availability of raw materials, economic viability, environmentally benign synthesis processes, and scalable production capabilities. By developing and optimizing such low-cost, environmentally friendly carbon material synthesis techniques, it is possible not only to reduce the production costs but also to facilitate the widespread application

of these materials across various fields (e.g., environmental, energy, and others).

5.3. Practical Application Challenges

1) Selectivity toward pollutants: Traditional treatment methods often lack the capability to address complex pollutants, such as persistent organic compounds or mixed organic compounds in wastewater. Therefore, materials with specific surface functional groups or pore structures are required for the selective adsorption and degradation of target pollutants. 2) Long-term operational stability: During actual wastewater treatment processes, electrodes may undergo passivation or catalyze side reactions due to impurities present in the wastewater sample, such as Cl^- ions and humic acid, leading to decreased catalytic activity. To address this issue, an in-depth investigation of passivation-resistant mechanisms and electrode regeneration methods is essential to ensure the lifetime of EAOP devices. 3) System integration and energy consumption: Despite demonstrating potential in the degradation of organic compounds, the high energy consumption associated with EAOPs restricts their feasibility for large-scale applications. To mitigate energy consumption, optimization of electrode structures (e.g., employing flow-through electrodes) or integration of EAOP with other technologies like photoelectrochemical catalysis and membrane separation can be effective strategies.

5.4. Potential Direction for Carbon-Based Materials in Next-Generation EAOPs and Current Challenges

Compared to Fe^{2+}/Fe^{3+}, quinone-based mediators exhibit several advantageous properties, including tunable redox potentials, a wide operational pH range, and the ability to facilitate electron transfer processes.[169] In the electro-Fenton system, utilizing the quinone/hydroquinone couple as an alternative to Fe^{2+}/Fe^{3+} can effectively prevent the issue caused by iron sludge and enhance the overall stability of the EAOP setup. This strategy represents a promising pathway for future EAOPs.

In addition to the above discussed EAOP device with an electrolyzer configuration, the galvanic cell configuration EAOP device represents a theoretically feasible alternative. This approach has been demonstrated in the Zn-air battery systems for the simultaneous generation of electricity and H_2O_2. Specifically, viologens[165] and phenazines[167] can be used as charge storage materials in the solution at the negative electrode, while carbon-based materials can serve as components of the positive electrode, facilitating the two-electron ORR and generating reactive radicals. When the device is activated, it can purify water while simultaneously producing electricity through the electrochemical reactions at both electrodes. This galvanic cell configuration enables the EAOP device to function outdoors without the need for an external power source. We believe that research into this type of device may represent a promising direction for the future development of EAOP technologies.

Given the current stage of development of carbon-based materials in EAOPs, their widespread implementation remains limited, and large-scale system evaluations are not yet feasible. Therefore, continued efforts are needed in the near future to promote the large-scale application. And, when scaling up EAOP setups, several critical challenges must be addressed, such as the durability of carbon-based materials and the energy consumption of EAOP equipment under real-world operating conditions.

In summary, significant challenges remain before EAOP systems can achieve widespread implementation. Additionally, carbon-based electrode materials require further optimization to meet energy-efficiency and economic-feasibility targets.

Acknowledgements

The authors gratefully acknowledge the funding from Sichuan Science and Technology Program (grant no. 2023ZYD0278), the funding from the National Key R&D Program of China (grant no. 2024YFA1509500), the support from Tianfu Yongxing Laboratory Organized Research Project Funding (grant no. 2024KFXM09), the funding from the National Natural Science Foundation of China (grant nos. 22479010 and 22275196), the funding from Sichuan University of Science & Engineering (grant no. 2024RC12), and the support of the Experimental Center of Advanced Materials at the Beijing Institute of Technology.

Conflict of Interest

The authors declare no conflict of interest.

Author Contributions

Zheng Tang: formal analysis (equal); investigation (equal); writing—original draft (equal); writing—review & editing (equal). **Yifan Zhang**: investigation (equal); writing—review & editing (equal). **Wulin Yang**: investigation (equal); writing—review & editing (equal). **Zipeng Zhao**: investigation (equal); writing—review & editing (equal). **Jincai Zhao**: investigation (equal); writing—review & editing (equal).

Keywords: carbon-based materials · electrochemical advanced oxidation processes · organic pollutant degradation · reactive oxygen species · redox flow batteries

[1] S. Anandan, V. Kumar Ponnusamy, M. Ashokkumar, *Ultrason. Sonochem.* **2020**, *67*, 105130.
[2] S. Garcia-Segura, E. Brillas, *J. Photochem. Photobiol., C* **2017**, *31*, 1.
[3] M. A. Oturan, J.-J. Aaron, *Crit. Rev. Env. Sci. Technol.* **2014**, *44*, 2577.
[4] J. Xie, J. Ma, C. Zhang, T. D. Waite, *Water Res.* **2021**, *203*, 117547.
[5] K. Zhang, Y. Zhang, S. Liu, X. Tong, J. Niu, J. C. Crittenden, *Int. J. Hydrogen Energy* **2024**, *71*, 473.
[6] S. O. Ganiyu, C. A. Martínez-Huitle, *Curr. Opin. Electrochem.* **2020**, *22*, 211.
[7] J. Radjenovic, D. L. Sedlak, *Environ. Sci. Technol.* **2015**, *49*, 11292.
[8] H. Yin, Q. Guo, C. Lei, W. Chen, B. Huang, *Chem. Eng. J.* **2020**, *396*, 125156.

[9] H. J. Lim, D. J. Kim, K. Rigby, W. Chen, H. Xu, X. Wu, J.-H. Kim, *Environ. Sci. Technol.* **2023**, *57*, 19054.
[10] Y. Liu, X. Yu, M. Kamali, X. Zhang, S. Feijoo, S. M. Al-Salem, R. Dewil, L. Appels, *Chem. Eng. J.* **2023**, *467*, 143291.
[11] Y. Guo, C. Tang, C. Cao, X. Hu, *Surf. Interfaces* **2023**, *38*, 102879.
[12] M. C. Santos, V. S. Antonin, F. M. Souza, L. R. Aveiro, V. S. Pinheiro, T. C. Gentil, T. S. Lima, J. P. C. Moura, C. R. Silva, L. E. B. Lucchetti, L. Codognoto, I. Robles, M. R. V. Lanza, *Chemosphere* **2022**, *307*, 135763.
[13] S. O. Ganiyu, M. Zhou, C. A. Martínez-Huitle, *Appl. Catal., B* **2018**, *235*, 103.
[14] B. P. Chaplin, *Environ. Sci. Processes Impacts* **2014**, *16*, 1182.
[15] J. Li, Y. Li, Z. Xiong, G. Yao, B. Lai, *Chin. Chem. Lett.* **2019**, *30*, 2139.
[16] Y. Shu, M. Hu, M. Zhou, H. Yin, P. Liu, H. Zhang, H. Zhao, *Mater. Chem. Front.* **2023**, *7*, 2528.
[17] M. El Kateb, C. Trellu, A. Darwich, M. Rivallin, M. Bechelany, S. Nagarajan, S. Lacour, N. Bellakhal, G. Lesage, M. Héran, M. Cretin, *Water Res.* **2019**, *162*, 446.
[18] A. Özcan, Y. Şahin, A. S. Koparal, M. A. Oturan, *Water Res.* **2008**, *42*, 2889.
[19] Y. Lin, J. Yu, Z. Xing, X. Guo, X. Yu, B. Tang, J. Zou, *Electrochim. Acta* **2016**, *213*, 341.
[20] X. Gao, H. Zhang, Y. Wang, H. Wang, Y. Tang, Y. Hu, Y. Lv, J. Bai, *Chem. Eng. J.* **2023**, *455*, 140696.
[21] P. Dong, H. Wang, W. Liu, S. Wang, Y. Wang, J. Zhang, F. Lin, Y. Wang, C. Zhao, X. Duan, S. Wang, H. Sun, *J. Hazard. Mater.* **2021**, *401*, 123423.
[22] F. Yu, L. Tao, Y. Yang, S. Wang, *Sep. Purif. Technol.* **2021**, *277*, 119432.
[23] E. Saputra, S. Muhammad, H. Sun, S. Wang, *RSC Adv.* **2013**, *3*, 21905.
[24] X. Wang, Q. Zhang, J. Jing, G. Song, M. Zhou, *Chem. Eng. J.* **2023**, *466*, 143283.
[25] H. Liu, W. Xiong, Y. Liu, G. Wang, C. Zhou, C. Lai, X. Huo, G. Zeng, M. Cheng, *Sep. Purif. Technol.* **2025**, *377*, 134397.
[26] C. Zhu, F. Liu, C. Ling, H. Jiang, H. Wu, A. Li, *Appl. Catal., B* **2019**, *242*, 238.
[27] S. Wang, Z. Tang, Z. Zhang, X. Fang, F. Li, *ACS ES&T Water* **2023**, *3*, 3544.
[28] L. Tian, M. Zhu, L.-S. Zhang, L.-J. Zhou, J.-P. Fan, D.-S. Wu, J.-P. Zou, *J. Environ. Chem. Eng.* **2022**, *10*, 107414.
[29] H. Ding, Y. Zhu, Y. Wu, J. Zhang, H. Deng, H. Zheng, Z. Liu, C. Zhao, *Environ. Sci. Technol.* **2020**, *54*, 10944.
[30] Y. Zhou, J. Jiang, Y. Gao, J. Ma, S.-Y. Pang, J. Li, X.-T. Lu, L.-P. Yuan, *Environ. Sci. Technol.* **2015**, *49*, 12941.
[31] H. Song, L. Yan, J. Jiang, J. Ma, S. Pang, X. Zhai, W. Zhang, D. Li, *Chem. Eng. J.* **2018**, *344*, 12.
[32] G. Divyapriya, P. V. Nidheesh, *Curr. Opin. Solid State Mater. Sci.* **2021**, *25*, 100921.
[33] J. E. Silveira, A. L. Garcia-Costa, T. O. Cardoso, J. A. Zazo, J. A. Casas, *Electrochim. Acta* **2017**, *258*, 927.
[34] J. Liu, S. Zhong, Y. Song, B. Wang, F. Zhang, *J. Electroanal. Chem.* **2018**, *809*, 74.
[35] G. Pan, Z. Sun, *Chemosphere* **2021**, *283*, 131257.
[36] J. Wang, C. Li, M. Rauf, H. Luo, X. Sun, Y. Jiang, *Sci. Total Environ.* **2021**, *759*, 143459.
[37] T. X. Huong Le, M. Bechelany, M. Cretin, *Carbon* **2017**, *122*, 564.
[38] A. Özcan, Y. Şahin, A. S. Koparal, M. A. Oturan, *Appl. Catal., B* **2009**, *89*, 620.
[39] E. Mousset, Z. T. Ko, M. Syafiq, Z. Wang, O. Lefebvre, *Electrochim. Acta* **2016**, *222*, 1628.
[40] E. Mousset, Z. Wang, J. Hammaker, O. Lefebvre, *Electrochim. Acta* **2017**, *258*, 607.
[41] Y. Sun, L. Silvioli, N. R. Sahraie, W. Ju, J. Li, A. Zitolo, S. Li, A. Bagger, L. Arnarson, X. Wang, T. Moeller, D. Bernsmeier, J. Rossmeisl, F. Jaouen, P. Strasser, *J. Am. Chem. Soc.* **2019**, *141*, 12372.
[42] S. O. Ganiyu, M. J. G. de Araújo, E. C. T. de Araújo Costa, J. E. L. Santos, *Appl. Catal., B* **2021**, *283*, 119652.
[43] L. Lyu, G. Yu, L. Zhang, C. Hu, Y. Sun, *Environ. Sci. Technol.* **2018**, *52*, 747.
[44] L. Tan, Y. Liu, G. Zhu, X. Fan, X. Quan, *Sci. Total Environ.* **2023**, *875*, 162725.
[45] F. Yu, L. Tao, T. Cao, *Environ. Pollut.* **2019**, *255*, 113119.
[46] L. Zhao, R. Zhu, H. Ma, X. Pan, X. Luo, X. Gong, *Sep. Purif. Technol.* **2024**, *347*, 127596.
[47] R. Kamaraj, N. Nesakumar, S. Vasudevan, *ChemistrySelect* **2020**, *5*, 10034.
[48] Y. Zhu, S. Qiu, F. Deng, F. Ma, Y. Zheng, *Sci. Total Environ.* **2020**, *722*, 137853.
[49] H. Zhao, S. Han, J. Jia, M. He, K. An, Z. Tang, S. Lai, X. Yang, Z. Wang, *Chem. Eng. J.* **2023**, *468*, 143505.
[50] F. Liu, Y. Liu, Q. Yao, Y. Wang, X. Fang, C. Shen, F. Li, M. Huang, Z. Wang, W. Sand, J. Xie, *Environ. Sci. Technol.* **2020**, *54*, 5913.
[51] J. E. S. van der Hoeven, J. Jelic, L. A. Olthof, G. Totarella, R. J. A. van Dijk-Moes, J.-M. Krafft, C. Louis, F. Studt, A. van Blaaderen, P. E. de Jongh, *Nat. Mater.* **2021**, *20*, 1216.
[52] X. Shen, F. Xiao, H. Zhao, Y. Chen, C. Fang, R. Xiao, W. Chu, G. Zhao, *Environ. Sci. Technol.* **2020**, *54*, 4564.
[53] M. Ye, C. Zhang, Z. Liu, H. Li, Z. Fu, H. Zhang, G. Wang, Y. Zhang, *Sep. Purif. Technol.* **2023**, *305*, 122507.
[54] W. Liu, C. Zhang, J. Zhang, X. Huang, M. Song, J. Li, F. He, H. Yang, J. Zhang, D. Wang, *Appl. Catal., B* **2022**, *310*, 121312.
[55] L. Yang, G. Sun, H. Fu, L. Zhang, *Chem. Eng. J.* **2023**, *472*, 145052.
[56] W. Zhang, J. W. Choi, S. Kim, T. T. Le, S. Nandy, C.-K. Hwang, S. Y. Paek, A. Byeon, K. H. Chae, S. Y. Lee, S. H. Kim, H. Song, J. Kim, J. Oh, J. W. Lee, S. S. Han, J. M. Kim, *Appl. Catal., B* **2023**, *331*, 122712.
[57] Y. Tian, W. Fu, Q. Wang, Y. Tang, M. Zhou, *Chem. Eng. J.* **2022**, *427*, 131694.
[58] P. Cao, X. Quan, K. Zhao, S. Chen, H. Yu, J. Niu, *J. Hazard. Mater.* **2020**, *382*, 121102.
[59] D. Ding, K. Shen, X. Chen, H. Chen, J. Chen, T. Fan, R. Wu, Y. Li, *ACS Catal.* **2018**, *8*, 7879.
[60] X. Chen, W. Teng, J. Fan, Y. Chen, Q. Ma, Y. Xue, C. Zhang, W.-x. Zhang, *J. Hazard. Mater.* **2022**, *427*, 127896.
[61] L. Chu, Z. Sun, G. Fang, L. Cang, X. Wang, D. Zhou, J. Gao, *Sep. Purif. Technol.* **2021**, *267*, 118680.
[62] X. Sun, H. Qi, Z. Sun, *Chemosphere* **2022**, *286*, 131972.
[63] P. Cao, K. Zhao, X. Quan, S. Chen, H. Yu, *Sep. Purif. Technol.* **2020**, *238*, 116424.
[64] D. Zhang, T. Liu, K. Yin, C. Liu, Y. Wei, *Chem. Eng. J.* **2020**, *383*, 123184.
[65] S. Ren, W. Cui, L. Li, Z. Yi, *Sustain. Energy Fuels* **2021**, *5*, 6310.
[66] C. Zhang, M. Ye, H. Li, Z. Liu, Z. Fu, H. Zhang, G. Wang, Y. Zhang, *Sep. Purif. Technol.* **2023**, *316*, 123778.
[67] L. Zhao, M. F. Murrieta, J. A. Padilla, S. Lanzalaco, P. L. Cabot, I. Sirés, *Sci. Total Environ.* **2024**, *953*, 176110.
[68] T. F. da Silva, P. S. Cavalheri, J. C. Cardoso, C. E. D. Nazario, J. Jorge, M. A. U. Martines, L. M. Ravaglia, G. B. Alcantara, G. A. Casagrande, A. R. L. Caires, R. P. Cavalcante, S. C. de Oliveira, F. Gozzi, I. Sirés, A. M. Junior, *Catal. Today* **2024**, *431*, 114579.
[69] K. Liu, M. Yu, H. Wang, J. Wang, W. Liu, M. R. Hoffmann, *Environ. Sci. Technol.* **2019**, *53*, 6474.
[70] Z. Ye, W. Zhang, S. Lanzalaco, L. Zhao, I. Sirés, P. Xia, J. Zhai, Q. He, *Chem. Eng. J.* **2023**, *455*, 140757.
[71] M. Liu, N. Li, S. Meng, S. Yang, B. Jing, J. Zhang, J. Jiang, S. Qiu, F. Deng, *J. Hazard. Mater.* **2024**, *478*, 135484.
[72] X. Du, W. Fu, P. Su, L. Su, Q. Zhang, J. Cai, M. Zhou, *ACS ES&T Eng.* **2021**, *1*, 1311.
[73] Z. Ye, J. A. Padilla, E. Xuriguera, E. Brillas, I. Sirés, *Appl. Catal., B* **2020**, *266*, 118604.
[74] X. Du, S. Wang, F. Ye, Z. Qingrui, *Environ. Res.* **2022**, *206*, 112414.
[75] Y. Li, T. Yang, S. Qiu, W. Lin, J. Yan, S. Fan, Q. Zhou, *Chem. Eng. J.* **2020**, *389*, 124382.
[76] J. Guo, G. Song, Y. Zheng, J. Gu, S. Li, M. Zhou, *Sep. Purif. Technol.* **2022**, *302*, 122141.
[77] X. Qin, P. Cao, X. Quan, K. Zhao, S. Chen, H. Yu, Y. Su, *Environ. Sci. Technol.* **2023**, *57*, 2907.
[78] R. Jinisha, R. Gandhimathi, S. T. Ramesh, P. V. Nidheesh, S. Velmathi, *Chemosphere* **2018**, *200*, 446.
[79] L. Lyu, L. Zhang, Q. Wang, Y. Nie, C. Hu, *Environ. Sci. Technol.* **2015**, *49*, 8639.
[80] H. Dong, H. Su, Z. Chen, H. Yu, H. Yu, *Electrochim. Acta* **2016**, *222*, 1501.
[81] E. Brillas, I. Sirés, M. A. Oturan, *Chem. Rev.* **2009**, *109*, 6570.
[82] X. Wang, H. Wu, J. Jing, G. Song, X. Zhang, M. Zhou, R. Dewil, *Green Energy Environ.* **2025**, *10*, 214.
[83] W. Yang, M. Zhou, L. Liang, *Chem. Eng. J.* **2018**, *338*, 700.
[84] X. Ren, H. Liu, J. Wang, J. Yu, *Chin. Chem. Lett.* **2024**, *35*, 109282.
[85] F. Yu, Y. Chen, Y. Pan, Y. Yang, H. Ma, *Sep. Purif. Technol.* **2020**, *241*, 116695.
[86] P. Su, M. Zhou, X. Lu, W. Yang, G. Ren, J. Cai, *Appl. Catal., B* **2019**, *245*, 583.
[87] W. Tian, H. Zhang, X. Duan, H. Sun, M. O. Tade, H. M. Ang, S. Wang, *ACS Appl. Mater. Interfaces* **2016**, *8*, 7184.
[88] J. Li, M. Xu, G. Yao, B. Lai, *Chem. Eng. J.* **2018**, *348*, 1012.
[89] L. Niu, G. Zhang, G. Xian, Z. Ren, T. Wei, Q. Li, Y. Zhang, Z. Zou, *Sep. Purif. Technol.* **2021**, *259*, 118156.

[90] Q. Yang, H. Choi, S. R. Al-Abed, D. D. Dionysiou, *Appl. Catal., B* **2009**, *88*, 462.
[91] J. C. Espinosa, P. Manickam-Periyaraman, F. Bernat-Quesada, S. Sivanesan, M. Álvaro, H. García, S. Navalón, *Appl. Catal., B* **2019**, *249*, 42.
[92] A. Shahzeydi, M. Ghiaci, L. Jameie, M. Panjepour, *Appl. Surf. Sci.* **2019**, *485*, 194.
[93] F. Sopaj, M. A. Rodrigo, N. Oturan, F. I. Podvorica, J. Pinson, M. A. Oturan, *Chem. Eng. J.* **2015**, *262*, 286.
[94] X. Zhao, Q.-D. An, Z.-Y. Xiao, S.-R. Zhai, Z. Shi, *Chem. Eng. J.* **2018**, *353*, 746.
[95] P. Lin, W. Zhu, Y. Gao, J. Li, J. Liu, J. Zhang, T. Huang, *Environ. Sci. Water Res. Technol.* **2022**, *8*, 62.
[96] J. Xie, X. Luo, L. Chen, X. Gong, L. Zhang, J. Tian, *Chem. Eng. J.* **2022**, *440*, 135760.
[97] Y. N. Liang, W.-D. Oh, Y. Li, X. Hu, *Appl. Catal., A* **2018**, *562*, 94.
[98] J. Peng, Z. Wang, S. Wang, J. Liu, Y. Zhang, B. Wang, Z. Gong, M. Wang, H. Dong, J. Shi, H. Liu, G. Yan, G. Liu, S. Gao, Z. Cao, *Chem. Eng. J.* **2021**, *409*, 128176.
[99] F. Xie, Q. Shi, H. Bai, M. Liu, J. Zhang, M. Qi, J. Zhang, Z. Li, W. Zhu, *Chemosphere* **2023**, *313*, 137384.
[100] Y. Liu, J. Wang, *Chem. Eng. J.* **2023**, *466*, 143147.
[101] Y. Wang, H. Zhao, G. Zhao, *Appl. Catal., B* **2015**, *164*, 396.
[102] J. Du, J. Bao, Y. Liu, S. H. Kim, D. D. Dionysiou, *Chem. Eng. J.* **2019**, *376*, 119193.
[103] Y. Xu, W. Li, J. Wang, D. Wu, N. Li, Y. Li, X. Fan, W. Peng, *Chemosphere* **2024**, *369*, 143885.
[104] S. Xin, B. Ma, C. Zhang, X. Ma, P. Xu, G. Zhang, M. Gao, Y. Xin, *Appl. Catal., B* **2021**, *294*, 120247.
[105] M. Cheng, Y. Zhang, B. Lai, L. Wang, S. Yang, K. Li, D. Wang, Y. Wu, G.-H. Chen, J. Qian, *Chem. Eng. J.* **2023**, *455*, 140615.
[106] A. Farhat, J. Keller, S. Tait, J. Radjenovic, *Environ. Sci. Technol.* **2015**, *49*, 14326.
[107] H. Song, L. Yan, J. Ma, J. Jiang, G. Cai, W. Zhang, Z. Zhang, J. Zhang, T. Yang, *Water Res.* **2017**, *116*, 182.
[108] X. Duan, S. Indrawirawan, H. Sun, S. Wang, *Catal. Today* **2015**, *249*, 184.
[109] X. Duan, H. Sun, S. Wang, *Acc. Chem. Res.* **2018**, *51*, 678.
[110] P. Su, W. Fu, Z. Hu, J. Jing, M. Zhou, *Appl. Catal., B* **2022**, *313*, 121457.
[111] S. Zhong, Z.-S. Zhu, P. Zhou, L. Shi, X. Duan, B. Lai, S. Wang, *ACS Appl. Nano Mater.* **2022**, *5*, 12095.
[112] Y. Wei, Y. Liu, T. Wang, G. Zhang, L. Yang, C. He, Z. Xiong, Z. Pan, B. Lai, *Sep. Purif. Technol.* **2024**, *328*, 125080.
[113] D. Wang, Y. Si, Y. Han, M. Xie, L. Xu, C. Sun, *Sep. Purif. Technol.* **2025**, *358*, 130256.
[114] G. Zhu, J. Zhu, Q. Liu, X. Fu, Z. Chen, K. Li, F. Cao, Q. Qin, M. Jiao, *Phys. Chem. Chem. Phys.* **2021**, *23*, 5283.
[115] M. Qi, P. Lin, Q. Shi, H. Bai, H. Zhang, W. Zhu, *Process Saf. Environ. Prot.* **2023**, *171*, 847.
[116] Y. Li, J. Yang, M. Zhang, Z. Yang, K. Shih, G.-G. Ying, Y. Feng, *Chem. Eng. J.* **2023**, *452*, 139484.
[117] Y. Liu, Y. Zhao, J. Wang, *Sci. Total Environ.* **2021**, *754*, 141883.
[118] S. Yang, W. Zhang, M. Liu, H. Zhao, H. Lu, H. Li, Z. Guo, A. Yuan, J. Yang, J. Pan, F. Yang, *A, J. Environ. Chem. Eng.* **2023**, *11*, 109190.
[119] M. S. Samuel, G. Kadarkarai, D. R. Ryan, S. T. McBeath, B. K. Mayer, P. J. McNamara, *Sci. Total Environ.* **2024**, *942*, 173736.
[120] B. Gao, L. Wu, S. Li, J. Yang, M. Dou, G. Chang, X. Li, *J. Hazard. Mater.* **2025**, *483*, 136698.
[121] Z. Zhou, M. Habib, Z. Xu, G. Zeng, R. Yang, Q. Sui, S. Lyu, *Sep. Purif. Technol.* **2024**, *334*, 126059.
[122] C. Han, X. Duan, M. Zhang, W. Fu, X. Duan, W. Ma, S. Liu, S. Wang, X. Zhou, *Carbon* **2019**, *153*, 73.
[123] P. Zhang, P. Zhou, J. Peng, Y. Liu, H. Zhang, C. He, Z. Xiong, W. Liu, B. Lai, *Water Res.* **2022**, *219*, 118626.
[124] K. Pei, S. Luo, F. He, J. Arbiol, Y. Xu, F. Zhu, Y. Wang, Y. Chen, *Appl. Catal., B* **2023**, *330*, 122601.
[125] G. Loget, A. Kuhn, *Nat. Commun.* **2011**, *2*, 535.
[126] Q. Guo, C. Lei, W. Chen, B. Huang, *ACS ES&T Water* **2023**, *3*, 2437.
[127] Z. Ge, X. Wang, X. Lei, W. Chen, Q. Guo, C. Lei, Y. Hu, Y.-G. Zhou, C. Feng, B. Huang, *Environ. Sci. Technol.* **2024**, *58*, 11843.
[128] Z. Sun, M. Gao, X. Yu, M. Wang, S. Wang, X. Wang, *J. Environ. Chem. Eng.* **2021**, *9*, 105694.
[129] I. Ali, A. Barros de Souza, D. Cabooter, S. De Laet, K. Van Eyck, R. Dewil, *Environ. Pollut.* **2023**, *334*, 122220.
[130] P. J. M. Cordeiro-Junior, A. S. Martins, G. B. S. Pereira, F. V. Rocha, M. A. R. Rodrigo, M. R. d. V. Lanza, *Sep. Purif. Technol.* **2022**, *285*, 120299.
[131] Q. Zhang, M. Zhou, Z. Lang, X. Du, J. Cai, L. Han, *Chem. Eng. J.* **2021**, *413*, 127564.
[132] M. G. Peleyeju, O. A. Arotiba, *Environ. Sci. Water Res. Technol.* **2018**, *4*, 1389.
[133] S. Kawrani, M. Boulos, M. F. Bekheet, R. Viter, A. A. Nada, W. Riedel, S. Roualdes, D. Cornu, M. Bechelany, *Appl. Surf. Sci.* **2020**, *516*, 146051.
[134] S. Kawrani, A. A. Nada, M. F. Bekheet, M. Boulos, R. Viter, S. Roualdes, P. Miele, D. Cornu, M. Bechelany, *Chem. Eng. J.* **2020**, *389*, 124326.
[135] R. Daghrir, P. Drogui, D. Robert, *J. Photochem. Photobiol., A* **2012**, *238*, 41.
[136] A. Miquelot, L. Youssef, C. Villeneuve-Faure, N. Prud'homme, N. Dragoe, A. Nada, V. Rouessac, S. Roualdes, J. Bassil, M. Zakhour, M. Nakhl, C. Vahlas, *J. Mater. Sci.* **2021**, *56*, 10458.
[137] B. O. Orimolade, O. A. Arotiba, *Electrocatalysis* **2019**, *10*, 429.
[138] Y. Zhou, X. Fan, G. Zhang, W. Dong, *Chem. Eng. J.* **2019**, *356*, 1003.
[139] B. A. Koiki, B. O. Orimolade, B. N. Zwane, D. Nkosi, N. Mabuba, O. A. Arotiba, *Electrochim. Acta* **2020**, *340*, 135944.
[140] M. Zhang, W. Pu, S. Pan, O. K. Okoth, C. Yang, J. Zhang, *J. Alloys Compd.* **2015**, *648*, 719.
[141] E. H. Umukoro, M. G. Peleyeju, J. C. Ngila, O. A. Arotiba, *Chem. Eng. J.* **2017**, *317*, 290.
[142] H.-J. Chen, Y.-L. Yang, M. Hong, J.-G. Chen, G.-Q. Suo, X.-J. Hou, L. Feng, Z.-G. Chen, *Sustain. Mater.Technol.* **2019**, *21*, e00105.
[143] A. A. Nada, B. O. Orimolade, H. H. El-Maghrabi, B. A. Koiki, M. Rivallin, M. F. Bekheet, R. Viter, D. Damberga, G. Lesage, I. Iatsunskyi, E. Coy, M. Cretin, O. A. Arotiba, M. Bechelany, *Appl. Mater. Today* **2021**, *24*, 101129.
[144] Z. Fan, H. Shi, H. Zhao, J. Cai, G. Zhao, *Carbon* **2018**, *126*, 279.
[145] B. O. Orimolade, B. A. Koiki, B. N. Zwane, G. M. Peleyeju, N. Mabuba, O. A. Arotiba, *RSC Adv.* **2019**, *9*, 16586.
[146] Y. Wang, H. Zhao, J. Gao, G. Zhao, Y. Zhang, Y. Zhang, *J. Phys. Chem. C.* **2012**, *116*, 7457.
[147] F. Marken, U. K. Sur, B. A. Coles, R. G. Compton, *Electrochim. Acta* **2006**, *51*, 2195.
[148] S. Ahn, M. Son, V. Singh, A. Yun, M.-H. Baik, H. R. Byon, *J. Am. Chem. Soc.* **2024**, *146*, 4521.
[149] Z. Wang, X. Liu, X. Zhang, H. Zhang, Y. Zhao, Y. Li, H. Yu, G. He, *Mater. Horiz.* **2024**, *11*, 1283.
[150] M. Hu, W. Wu, J. Luo, T. L. Liu, *Adv. Energy Mater.* **2022**, *12*, 2202085.
[151] J. Gao, L. Xia, M. Ou, Z. a. Tan, *Batteries Supercaps* **2024**, *7*, e202400434.
[152] J. Moutet, D. D. Mills, D. L. Lozier, T. L. Gianetti, *Batteries Supercaps* **2024**, *7*, e202300519.
[153] L. A. Robertson, I. A. Shkrob, Z. Li, G. Agarwal, Z. Yu, R. S. Assary, L. Cheng, L. Zhang, Z. Zhang, *Batteries Supercaps* **2025**, *8*, e202400597.
[154] E. Bai, C. Sun, H. Zhu, Z. Liu, C. Xu, X. Xie, S. Wu, *Batteries Supercaps* **2024**, *7*, e202400007.
[155] M. Shoaib, P. Vallayil, N. Jaiswal, P. Iyapazham Vaigunda Suba, S. Sankararaman, K. Ramanujam, V. Thangadurai, *Adv. Energy Mater.* **2024**, *14*, 2400721.
[156] W. Wu, L. Huang, Y. Li, M. Li, Y. Chen, Y. Yang, X. Chen, Y. Wu, L. Gu, X. Cao, *Adv. Mater. Technol.* **2022**, *7*, 2100708.
[157] Z. Deng, M. Gong, Z. Gong, X. Wang, *Nano Lett.* **2022**, *22*, 9551.
[158] M. R. Mohamed, P. K. Leung, M. H. Sulaiman, *Appl. Energy* **2015**, *137*, 402.
[159] P. K. Leung, C. Ponce-de-León, C. T. J. Low, A. A. Shah, F. C. Walsh, *J. Power Sources* **2011**, *196*, 5174.
[160] P. K. Leung, M. R. Mohamed, A. A. Shah, Q. Xu, M. B. Conde-Duran, *J. Power Sources* **2015**, *274*, 651.
[161] P. Leung, J. Palma, E. Garcia-Quismondo, L. Sanz, M. R. Mohamed, M. Anderson, *J. Power Sources* **2016**, *310*, 1.
[162] J. Winsberg, T. Hagemann, T. Janoschka, M. D. Hager, U. S. Schubert, *Angew. Chem. Int. Ed.* **2017**, *56*, 686.
[163] C. S. Sevov, D. P. Hickey, M. E. Cook, S. G. Robinson, S. Barnett, S. D. Minteer, M. S. Sigman, M. S. Sanford, *J. Am. Chem. Soc.* **2017**, *139*, 2924.
[164] Y. Ji, M.-A. Goulet, D. A. Pollack, D. G. Kwabi, S. Jin, D. De Porcellinis, E. F. Kerr, R. G. Gordon, M. J. Aziz, *Adv. Energy Mater.* **2019**, *9*, 1900039.
[165] C. DeBruler, B. Hu, J. Moss, J. Luo, T. L. Liu, *ACS Energy Lett.* **2018**, *3*, 663.

[166] K. Lin, R. Gómez-Bombarelli, E. S. Beh, L. Tong, Q. Chen, A. Valle, A. Aspuru-Guzik, M. J. Aziz, R. G. Gordon, *Nat. Energy* **2016**, *1*, 16102.
[167] A. Hollas, X. Wei, V. Murugesan, Z. Nie, B. Li, D. Reed, J. Liu, V. Sprenkle, W. Wang, *Nat. Energy* **2018**, *3*, 508.
[168] H. Li, H. Fan, B. Hu, L. Hu, G. Chang, J. Song, *Angew. Chem. Int. Ed.* **2021**, *60*, 26971.
[169] B. Huskinson, M. P. Marshak, C. Suh, S. Er, M. R. Gerhardt, C. J. Galvin, X. Chen, A. Aspuru-Guzik, R. G. Gordon, M. J. Aziz, *Nature* **2014**, *505*, 195.
[170] C.-S. Lee, T. H. Jeon, Y. H. Jang, H. J. Lim, B. J. Kwon, O. Kwon, K. Kumar, N. Sunariwal, T. Kim, *Chem. Eng. J.* **2024**, *481*, 148431.

Manuscript received: May 9, 2025
Revised manuscript received: July 17, 2025
Version of record online: